Semiclassical transport with Berry curvature: Chambers formula and applications to systems with Fermi surface topological transitions

Emmanouil K. Kokkinis,[1,2] Garry Goldstein,[3] Dmitri V. Efremov,[1,4] and Joseph J. Betouras[1]
[1]*Department of Physics, Loughborough University, Loughborough LE11 3TU, United Kingdom*
[2]*Physics Department, University of Crete, Heraklion 71003, Greece*
[3]*Physics Department, Boston University, Boston, Massachusetts 02215, USA*
[4]*IFW Leibniz Institute for Solid State and Materials Research, Dresden, Helmholtz str. 20, 01069 Dresden, Germany*

(Received 28 November 2021; revised 20 March 2022; accepted 4 April 2022; published 14 April 2022)

Starting with general semiclassical equations of motion for electrons in the presence of electric and magnetic fields, we extend the Chambers formula to include, in addition to a magnetic field, time-dependent electric fields, and bands with Berry curvature. We thereby compute the conductivity tensor $\sigma_{\alpha\beta}(B,\omega)$ in the presence of magnetic field for bands in two (2D) and three (3D) dimensions with Berry curvature. We focus then on several applications to magnetotransport for metals with Fermi surface topological transitions in 2D. In particular, we consider a rectangular lattice and a model related to overdoped graphene, to investigate the signatures of different types of Fermi surface topological transitions in metals in the Hall coefficient, Hall conductivity σ_{xy}, and longitudinal conductivity σ_{xx}. The behavior of those quantities as a function of frequency, when the electric field is time dependent, is also investigated. As an example of nonzero Berry curvature, we study the magnetotransport of the Haldane model within this context. In addition, we provide the linear and nonlinear electric current formula to order E^2.

DOI: 10.1103/PhysRevB.105.155123

I. INTRODUCTION

The majority of metals are well described by the Fermi liquid theory. Within this formalism the classical Hall effect arises due to the electron path curvature in the presence of an external magnetic fields [1]. It is characterized by the Hall coefficient $R_H = E_y/(j_x B_z)$, where j_x is the current density perpendicular to the applied magnetic field B_z and E_y is the induced electric field. In the case of a single band the Hall coefficient depends only on the sign of the charge and the density of the carriers. Therefore the Hall coefficient at zero temperature is widely used as a measure of the number of electrons or holes enclosed in a closed orbit [1,2]. However, the Hall coefficient may deviate from the simple form of counting of the number of electrons or holes enclosed in the electron-and hole-like pockets. It happens, e.g., in multiband systems and in the systems close to the Fermi surface topological transitions (FSTTs), as they are connected to singularities in the density of states, called Van Hove singularities [3–6].

There have been extensive studies of Lifshitz transitions (pocket appearing/disappearing or neck formation/collapse) and associated Van Hove singularities in a variety of materials including cuprates, iron based superconductors, cobaltates, Sr_2RuO_4, and heavy fermions [7–17]. Most of these materials show logarithic-type Van Hove singularity, which corresponds to a logarithmic singularity of the density of states at the Lifshitz transition in 2D. However, there is a recent surge of interest in higher order Van Hove singularities, which manifest itself in the stronger than logarithmic singularity in the density of states. These are the result of more complicated FSTTs. A prominent example is $Sr_3Ru_2O_7$, where a $n = 4$ Van Hove singularity connected to a more complicated FSST, is shown to exist in the presence of an external magnetic field [18]. Higher order Van Hove saddle points has been observed in highly overdoped graphene and twisted bilayer graphene [19–22] and may be highly relevant for the recently observed phases of Bernal bilayer graphene [23,24].

In this paper, we study the evolution of the Hall coefficient across a FSTT that correspond to a high-order Van Hove singularities using the Boltzman equation in the presence of a static magnetic field, a Berry curvature $\mathbf{\Omega}(\mathbf{k})$ and a low-frequency electric field $\mathbf{E}(\mathbf{r},t) = \mathbf{E}(\mathbf{r})\exp(i\omega t)$. The solution of the Boltzmann equation is provided in form of the Chambers formula [25], which is widely used in studies of the magnetotransport [1,2,26–34]. We extend the Chambers formula to the case of Berry curvature.

The equations of motion used in this paper are correct to leading order in the electric field E and magnetic field B, but remarkably, retain the same form when corrected to order E^2 and B^2 [35,36]. However, using the methods presented here it is possible to study the Boltzmann equation for arbitrary magnetic fields and electric fields with sufficiently accurate equations of motion [35]. To illustrate this idea we use the leading order equations of motion to study the solution to the Boltzmann equation in the magnetic field B and to quadratic order in the electric field E^2 (within the leading order equations of motion). We ignore the Zeeman splitting and consider spinless fermions thereby reducing to the case of negligible spin orbit coupling [35–39], thus avoiding more complicated

expressions [40]. We also neglect any changes to the chemical potential due to the magnetic field, these can be incorporated straightforwardly [35–39].

The main contributions of this paper are: (i) short and clear derivations of the Boltzmann equation relevant to the semiclassical motion of Fermi liquids, including the Berry curvature for leading order equations of motion; (ii) explicit solution of that Boltzmann equation to all orders in the magnetic and electric fields (formally exact), which can be implemented numerically for leading order equations of motion; (iii) method for semi-analytical asymptotic expansions of the Boltzmann equation solution to all orders in magnetic field and to an arbitrary (finite) order in the electric field for any set of equations of motion; and (iv) explicit expansion of Boltzmann equation solution to linear and quadratic orders in the electric field with Berry curvature using the developed method, thus obtaining linear and bilinear response (recently introduced in Refs. [41,42]), using the leading order equations of motion.

It is worth emphasizing that the paper is valid within the different Fermi surface topologies but away from the transition points. At the transition points, as the Fermi velocity approaches zero, quantum effects become important as well as possible out-of-equilibrium effects in a time-dependent electric field. In particular magnetic breakdown quantum description of field-induced tunneling between semiclassical orbits shall be considered carefully close to Van Hove singularities [43,44].

The rest of the paper is organized as follows: In Sec. II we review the semiclassical equations of motion in the presence of external fields and Berry curvature, as well as the Boltzmann equation that follows. In Sec. III we derive the new 2D and 3D version of the Chambers formula with Berry curvature and time dependent external electrical field. In Secs. IV–VI we apply these results to specific classes of materials. In Sec. IV we discuss the case of a Lifshitz transition of the form neck formation/collapse verifying that the rapid change between electron like to hole like Fermi surfaces leads to a rapid change of the Hall coefficient, which we also study as a function of frequency. In Sec. V we present the application to FSTT that corresponds to a higher Van Hove saddle in graphene and show how different FS topologies lead to different responses in conductivities. In Sec. VI we study the Hall conductivity of the Haldane model, as a representative example of a system with Berry curvature. In Sec. VII we conclude.

II. SEMICLASSICAL EQUATIONS OF MOTION - BOLTZMANN EQUATION AND SOLUTION

The semiclassical equations of motion for electrons of a single particle Hamiltonian $H(k)$ to leading order in electric and magnetic fields was discussed in numerous works [35,37–39,45–49] and can be written as

$$\frac{d\mathbf{r}}{dt} = D^{-1}(\mathbf{r},\mathbf{k},t)[\nabla_{\mathbf{k}}\varepsilon_M(\mathbf{k}) + e\mathbf{E}(\mathbf{r},t)\times\mathbf{\Omega}(\mathbf{k}) + e(\mathbf{\Omega}(\mathbf{k})\cdot\nabla_{\mathbf{k}}\varepsilon_M(\mathbf{k}))\mathbf{B}(\mathbf{r},t)], \quad (1)$$

$$\frac{d\mathbf{k}}{dt} = -D^{-1}(\mathbf{r},\mathbf{k},t)[e\mathbf{E}(\mathbf{r},t) + e\nabla_{\mathbf{k}}\varepsilon_M(\mathbf{k})\times\mathbf{B}(\mathbf{r},t) + e^2(\mathbf{B}(\mathbf{r},t)\cdot\mathbf{E}(\mathbf{r},t))\mathbf{\Omega}(\mathbf{k})]. \quad (2)$$

Here we have introduced $D^{-1}(\mathbf{r},\mathbf{k},t) = \frac{1}{1+e\mathbf{B}(\mathbf{r},t)\cdot\mathbf{\Omega}(\mathbf{k})}$. The Berry curvature $\mathbf{\Omega}(\mathbf{k})$ is defined as the pseudovector $\mathbf{\Omega}(\mathbf{k}) = \nabla_{\mathbf{k}}\times\mathcal{A}(\mathbf{k})$, where $\mathcal{A}(\mathbf{k}) = i\langle u(\mathbf{k})|\nabla_{\mathbf{k}}|u(\mathbf{k})\rangle$ is the Berry connection and $|u(\mathbf{k})\rangle$ an eigenstate of the Hamiltonian $H(\mathbf{k})$. The electron dispersion up to the second order of the magnetic fields can be written as [37,38]

$$\varepsilon_M(\mathbf{k}) = \varepsilon(\mathbf{k}) - \mathbf{m}(\mathbf{k})\cdot\mathbf{B}$$

with

$$\mathbf{m}(\mathbf{k}) = -i\frac{e}{2\hbar}\langle\nabla_{\mathbf{k}}u|\times[H(\mathbf{k})-\varepsilon(\mathbf{k})]|\nabla_{\mathbf{k}}u\rangle. \quad (3)$$

For simplicity, we consider below two dimensional (2D) case with both the electric and magnetic fields being uniform. Furthermore we consider time-independent magnetic field along z axis (which in 2D is out of plane). The electric field is taken weakly time dependent, that we can neglect the induction of the magnetic field. In two dimensions (2D), the Berry curvature is perpendicular to the plane $\Omega_z(\mathbf{k}) = \partial_{k_x}\mathcal{A}_y - \partial_{k_y}\mathcal{A}_x = -2\,\mathrm{Im}\langle\partial_{k_x}u \mid \partial_{k_y}u\rangle$ and $\mathbf{\Omega}(\mathbf{k})\cdot\nabla_{\mathbf{k}}\varepsilon_M(\mathbf{k}) = 0$. This configuration considerably simplifies the set of Eqs. (1)–(2).

Now we derive of the Boltzmann equation for our case. The derivation is the same in 2D or 3D so the dimensionality will be denoted by d and we will distinguish the differences in the next subsections. Let us take a small volume in phase space then the total number of particles in the system satisfies the continuity equation [35,45,50,51]:

$$\frac{\partial[Df]}{\partial t} + \nabla\cdot(\mathbf{w}Df) = \frac{D}{\tau_S(\mathbf{k})}(f_0 - f), \quad (4)$$

where $f = f(\mathbf{k},\mathbf{r},t)$ is the distribution of electrons while $f_0 = f_0(\varepsilon_M(\mathbf{k}))$ is the Fermi-Dirac distribution, $\tau_S(\mathbf{k})$ is the relaxation time and $\mathbf{w} = (\frac{d\mathbf{r}}{dt}, \frac{d\mathbf{k}}{dt})$, $\nabla = (\nabla_{\mathbf{r}}, \nabla_{\mathbf{k}})$ is the six velocity in phase space. Using the identity [38,50]

$$\nabla\cdot\mathbf{w} = -\frac{d}{dt}\ln(D(\mathbf{k},\mathbf{r},t)) = -\frac{\partial}{\partial t}\ln(D(\mathbf{k},\mathbf{r},t)) - \mathbf{w}\cdot\nabla\ln(D(\mathbf{k},\mathbf{r},t)) \quad (5)$$

we obtain the Boltzmann equation for the distribution of electrons:

$$\frac{\partial}{\partial t}[f(\mathbf{k},\mathbf{r},t)] + \mathbf{w}\cdot\nabla[f(\mathbf{k},\mathbf{r},t)] = \frac{[f_0(\varepsilon_M) - f(\mathbf{k},\mathbf{r},t)]}{\tau_S(\mathbf{k})} \quad (6)$$

with $\frac{d\mathbf{k}}{dt}$ and $\frac{d\mathbf{r}}{dt}$ being given by Eq. (2). By considering spatially uniform magnetic and electric fields, the equation becomes

$$\frac{\partial f}{\partial t} + \frac{d\mathbf{k}}{dt}\frac{df}{d\mathbf{k}} = -\frac{1}{\tau_S(\mathbf{k})}(f - f_0(\varepsilon_{\mathbf{M}})). \quad (7)$$

The solution to Eq. (7) is given by [52]

$$f(\mathbf{k},t) = f(\mathbf{k_0},t_0)\exp\left(-\int_{t_0}^{t}\frac{ds}{\tau_S(\mathbf{k}(s))}\right) + \int_{t_0}^{t} ds \frac{f_0\{\varepsilon_M[\mathbf{k}(s)]\}}{\tau_S(\mathbf{k}(s))}\exp\left(-\int_s^t \frac{dt'}{\tau_S(\mathbf{k}(t'))}\right). \quad (8)$$

In the above $f(\mathbf{k}_0, t_0)$ corresponds to the initial conditions. The components of the current density are given by

$$J_\alpha(t) = -e\int D(\mathbf{k})\frac{d^dk}{(2\pi)^d}\frac{dr_\alpha}{dt}f(\mathbf{k},t), \quad (9)$$

where the volume V of the unit cell of the lattice is set to unity and $d = 2, 3$ is the dimensionality of the system. If the initial time is set to $t_0 \to -\infty$ then

$$f(\mathbf{k},t) = \int_{-\infty}^{t} ds \frac{f_0\{\varepsilon_M[\mathbf{k}(s)]\}}{\tau_S(\mathbf{k}(s))}\exp\left(-\int_s^t \frac{dt'}{\tau_S(\mathbf{k}(t'))}\right) \quad (10)$$

and we note if we further linearize Eq. (10) we recover the linear response equations.

III. GENERAL RESULTS

We first present here the general formulas, while the derivations are left for the Appendix B. The 2D and 3D cases are treated separately, due to the differences in the equations of motion Eq. (2), when the Berry curvature is taken into account. As stressed in the introduction, the formulas are exact within the accuracy of the leading order equations of motion in the fields E and B.

A. Three-dimensional case

To find $\mathbf{k}(t)$, the equation of motion is given by Eq. (2). In the limit where $\mathbf{E}(t)$ is small, the last term of Eq. (2) can be taken as a perturbation. In that spirit let us denote by $\mathbf{k}_0(t)$ the solution to the equation:

$$\frac{d\mathbf{k}_0(t)}{dt} = -eD^{-1}(\mathbf{k}_0)[\nabla_{\mathbf{k}}\varepsilon_M(\mathbf{k}(t))\times\mathbf{B}]_{\mathbf{k}=\mathbf{k_0}} \quad (11)$$

and write: $\mathbf{E}(t) = \lambda\mathbf{E}(t)$ with $\lambda = 1$. Then Eq. (2) becomes analytically dependent on the parameter λ and its solutions can be written as an analytic asymptotic series of the form [53–55]:

$$\mathbf{k}(t) = \mathbf{k}_0(t) + \lambda\mathbf{k}_1(t) + \lambda^2\mathbf{k}_2(t) + \cdots \quad (12)$$

with $\mathbf{k}_1(t_0) = \mathbf{k}_2(t_0) = \mathbf{k}_3(t_0) = \cdots = 0$.. These expansions and the method below are valid to any accuracy with respect to the external fields in the equations of motion. To order λ:

$$\frac{d\mathbf{k}_1(t)}{dt} = -e\sum_\beta k_{1\beta}(t)\left[\frac{\partial}{\partial k_\beta}\left(D^{-1}(\mathbf{k})[\nabla_{\mathbf{k}}\varepsilon_M(\mathbf{k}(t))\times\mathbf{B}]\right)\right]_{\mathbf{k}=\mathbf{k}_0} - eD^{-1}(\mathbf{k}_0(t))[\mathbf{E}(t) + e(\mathbf{B}\cdot\mathbf{E}(t))\boldsymbol{\Omega}(\mathbf{k}_0(t))]. \quad (13)$$

Taking into account that $\frac{d\varepsilon(\mathbf{k}(t))}{dt} = \nabla_{\mathbf{k}}\varepsilon(\mathbf{k}(t))\cdot\frac{d\mathbf{k}}{dt}$, we can also write perturbatively:

$$\varepsilon_M(t) = \varepsilon_0(t) + \lambda\varepsilon_1(t) + \lambda^2\varepsilon_2(t) + \cdots \quad (14)$$

with $\varepsilon_0(t_0) = \varepsilon_M(t_0)$ and $\varepsilon_1(t_0) = \varepsilon_2(t_0) = \varepsilon_3(t_0) = \cdots = 0$. Again this is valid for any accuracy of the equations of motion. Then to order λ and for $t > t_0$:

$$\varepsilon_1(t) = e\int_{t_0}^{t} ds D^{-1}(\mathbf{k}_0(s)) \times[\nabla_{\mathbf{k}}\varepsilon_M(\mathbf{k}(s))\cdot(\mathbf{E}(s) + (\mathbf{B}\cdot\mathbf{E}(s))\boldsymbol{\Omega}(\mathbf{k}(s)))]_{\mathbf{k}=\mathbf{k_0}}$$

and to order λ^2

$$\varepsilon_2(t) = e\int_{t_0}^{t} ds\sum_{\alpha\beta}E_\beta(s)k_{1\alpha}(s)\frac{\partial}{\partial k_\alpha}\Bigg[D^{-1}(\mathbf{k}_0(s)) \times\left[\frac{\partial}{\partial k_\beta}\varepsilon_M(\mathbf{k}(s)) + eB_\beta(\nabla_{\mathbf{k}}\varepsilon_M(\mathbf{k}(s))\cdot\boldsymbol{\Omega}(\mathbf{k}(s)))\right]\Bigg]_{\mathbf{k}=\mathbf{k_0}}$$

We introduce for convenience the quantities:

$$\mathbf{u_0}(\mathbf{k}) \equiv D^{-1}(\mathbf{k})[\nabla_{\mathbf{k}}\varepsilon_M(\mathbf{k}) + e(\boldsymbol{\Omega}(\mathbf{k})\cdot\nabla_{\mathbf{k}}\varepsilon_M(\mathbf{k}))\mathbf{B}]$$

$$\eta(t;t_0) \equiv \exp\left(-\int_{t_0}^{t}\frac{ds}{\tau_S(\mathbf{k}_0(s))}\right)$$

As a result, we obtain the current to linear order in E:

$$J_\alpha^{(1)}(t) = -e^2\int\frac{d^3k}{(2\pi)^3}[\mathbf{E}(t)\times\boldsymbol{\Omega}(\mathbf{k})]_\alpha f_0\{\varepsilon_M[\mathbf{k}(t)]\} - e\int\frac{d^3k}{(2\pi)^3}D(\mathbf{k})u_{0\alpha}(\mathbf{k})\frac{\partial f_0\{\varepsilon_M[\mathbf{k}_0(t)]\}}{\partial\varepsilon} \times\int_{-\infty}^{t} D^{-1}(\mathbf{k}_0(t'))\nabla_{\mathbf{k}}\varepsilon(\mathbf{k}_0(t'))\cdot[\mathbf{E}(t') + e(\mathbf{B}\cdot\mathbf{E}(t'))\boldsymbol{\Omega}(\mathbf{k}_0(t'))]\eta(t;t')dt' \quad (15)$$

where the first term generalizes the Streda formula [37], while the second term generalizes the Chambers formula [25]. Next, to order E^2 we obtain

$$J_\alpha^{(2)}(t) = -e\int\frac{d^3k}{(2\pi)^3}D(\mathbf{k})u_{0\alpha}(\mathbf{k})\Bigg[e\frac{\partial f_0\{\varepsilon[\mathbf{k}_0(t)]\}}{\partial\varepsilon}\int_{-\infty}^{t}dt'\sum_\gamma k_{1\gamma}(t')\frac{\partial}{\partial k_\gamma}[D^{-1}(\mathbf{k}_0(t'))[\nabla_{\mathbf{k}}\varepsilon(\mathbf{k}_0(t'))\cdot[\mathbf{E}(t') + e(\mathbf{B}\cdot\mathbf{E}(t'))\boldsymbol{\Omega}(\mathbf{k}_0(t'))]]\eta(t;t') + e^2\frac{\partial^2 f_0\{\varepsilon[\mathbf{k}_0(t)]\}}{\partial\varepsilon^2}\int_{-\infty}^{t}dt'D^{-1}(\mathbf{k}_0(t'))\nabla_{\mathbf{k}}\varepsilon(\mathbf{k}_0(t'))\cdot[\mathbf{E}(t) + e(\mathbf{B}\cdot\mathbf{E}(t'))\boldsymbol{\Omega}(\mathbf{k}_0(t'))] \times\eta(t;t')\int_{t'}^{t}dlD^{-1}(\mathbf{k}_0(l))\nabla_{\mathbf{k}}\varepsilon(\mathbf{k}_0(l))\cdot[\mathbf{E}(l) + e(\mathbf{B}\cdot\mathbf{E}(l))\boldsymbol{\Omega}(\mathbf{k}_0(l))] + e\frac{\partial f_0\{\varepsilon[\mathbf{k}_0(t)]\}}{\partial\varepsilon}$$

$$\times \int_{-\infty}^{t} dt' D^{-1}(\mathbf{k}_0(t'))\nabla_{\mathbf{k}}\varepsilon(\mathbf{k}_0(t'))\cdot[\mathbf{E}(t')+e(\mathbf{B}\cdot\mathbf{E}(t'))\boldsymbol{\Omega}(\mathbf{k}_0(t'))]\eta(t;t')\int_{t'}^{t} dl\,\frac{\nabla_{\mathbf{k}}\tau_S(\mathbf{k}_0(l))\cdot\mathbf{k}_1(l)}{\tau_S^2(\mathbf{k}_0(l))}\Bigg]$$

$$-e^3\int\frac{d^3k}{(2\pi)^3}[\mathbf{E}(t)\times\boldsymbol{\Omega}(\mathbf{k})]_\alpha\frac{\partial f_0(\varepsilon(\mathbf{k}))}{\partial\varepsilon}\int_{-\infty}^{t} dt' D^{-1}(\mathbf{k}_0(t'))\nabla_{\mathbf{k}}\varepsilon(\mathbf{k}_0(t'))\cdot[\mathbf{E}(t')+e(\mathbf{B}\cdot\mathbf{E}(t'))\boldsymbol{\Omega}(\mathbf{k}_0(t'))]\eta(t;t'). \quad (16)$$

The first term is a shift of the Fermi-Dirac distribution due to the electric field, the second term is the quadratic shift, the third term is a novel one that corresponds to a nonconstant relaxation time and the last term generalizes the Berry dipole introduced in [41,42] to potentially any magnetic field and electric fields with arbitrary time dependence. As it is explained in Appendix D, it is important in order convergence to be guaranteed, that the eigenvalues of the matrix:

$$M_{\alpha\beta}(s)=-e\sum_{\gamma\delta}\varepsilon_{\alpha\gamma\delta}B_\delta\frac{\partial}{\partial k_\beta}\left[D^{-1}(\mathbf{k}_0(s))\left[\frac{\partial}{\partial k_\gamma}\varepsilon_M(\mathbf{k}_0(s))\right]\right]$$

is smaller than $\frac{1}{\tau_S(\mathbf{k})}$.

B. Two-dimensional case

We can now reduce all previous results to 2D. The equation of motion reads:

$$\frac{d\mathbf{k}}{dt}=-D^{-1}(\mathbf{r},\mathbf{k},t)(e\mathbf{E}(t)+e\nabla_{\mathbf{k}}\varepsilon_M(\mathbf{k})\times\mathbf{B}). \quad (17)$$

If we introduce for convenience the notation:

$$\mathbf{u_0^{2D}}(\mathbf{k})=D^{-1}(\mathbf{k})\nabla_{\mathbf{k}}\varepsilon_M(\mathbf{k}), \quad (18)$$

we arrive at a similar expression for the current as Eqs. (15) and (16) with the only differences that $\mathbf{u_0}$ is replaced by $\mathbf{u_0^{2D}}$, the integration over all $\mathbf{k}$'s is now a 2D integration and $\mathbf{B}\cdot\mathbf{E}(t)\to 0$. The result for the linear response is

$$J_\alpha^{(1)}(t)=-e^2\int\frac{d^2k}{(2\pi)^2}[\mathbf{E}(t)\times\boldsymbol{\Omega}(\mathbf{k})]_\alpha f_0\{\varepsilon_M[\mathbf{k}(t)]\}$$
$$-e^2\int\frac{d^2k}{(2\pi)^2}D(\mathbf{k})\mathbf{u}_{0\alpha}^{\mathbf{2D}}(\mathbf{k})\frac{\partial f_0\{\varepsilon_M[\mathbf{k}_0(t)]\}}{\partial\varepsilon}$$
$$\times\int_{-\infty}^{t} D^{-1}(\mathbf{k}_0(t'))\nabla_{\mathbf{k}}\varepsilon(\mathbf{k}_0(t'))\cdot\mathbf{E}(t')\eta(t;t')dt'. \quad (19)$$

For completeness we include the formula for the nonlinear response in 2D in the Appendix (B3) and we proceed to the scaling analysis below.

1. Scaling analysis in 2D

From the expression of the current we obtain the expression of the conductivity, which is divided into a part that we call topological and a regular part:

$$\sigma_{\alpha\beta}(e,\tau_S,T,\mathbf{B},\omega,\varepsilon_M)=-e^2\int\frac{d^2k}{(2\pi)^2}\varepsilon_{\alpha\beta}\Omega(\mathbf{k})f_{0T}\{\varepsilon_M[\mathbf{k}(t)]\}-e\int\frac{d^2k}{(2\pi)^2}\nabla_{\mathbf{k}_\alpha}\varepsilon_M(\mathbf{k})\frac{\partial f_{0T}\{\varepsilon_M[\mathbf{k}_0(t)]\}}{\partial\varepsilon}$$
$$\times\int_{-\infty}^{t} dt' D^{-1}(\mathbf{k}_0(t))\nabla_{\mathbf{k}_\beta}\varepsilon_M(\mathbf{k}_0(t'))\cdot\exp(i\omega(t'-t))\exp(-(t-t')/\tau_S) \quad (20)$$

with $\sigma_{\alpha\beta}^{\text{top}}(e,\tau_S,T,\mathbf{B},\omega,\varepsilon_M)=-e^2\int\frac{d^2k}{(2\pi)^2}\varepsilon_{\alpha\beta}\Omega(\mathbf{k})f_{0T}(\varepsilon_M(\mathbf{k}(t)))$ and

$$\sigma_{\alpha\beta}^{reg}(e,\tau_S,T,\mathbf{B},\omega,\varepsilon_M)=-e\int\frac{d^2k}{(2\pi)^2}\nabla_{k_\alpha}\varepsilon_M(\mathbf{k})\frac{\partial f_{0T}\{\varepsilon_M[\mathbf{k}_0(t)]\}}{\partial\varepsilon}$$
$$\times\int_{-\infty}^{t} dt' D^{-1}(\mathbf{k}_0(t'))\nabla_{k_\beta}\varepsilon_M(\mathbf{k}_0(t'))\cdot\exp(i\omega(t'-t))\exp(-(t-t')/\tau_S) \quad (21)$$

Where we assume a constant relaxation time τ_S. By introducing $\mathcal{B}=eB$, $\tilde{t}=(t'-t)/\tau_S$, $\mathcal{E}_M=\tau_S\varepsilon_M$, $\tilde{\omega}=\omega\tau_S$ and taking into account the equations of motion, we obtain for the regular part of the conductivity:

$$\sigma_{\alpha\beta}^{reg}(e,\tau_S,T,\mathbf{B},\omega,\varepsilon_M)=-e\tau_S^{-1}\int\frac{d^2k}{(2\pi)^2}\nabla_{\mathbf{k}_\alpha}\mathcal{E}_M(\mathbf{k})\frac{\partial f_{0T\tau_S}(\mathcal{E}_M(\mathbf{k}))}{\partial\mathcal{E}}$$
$$\times\int_{-\infty}^{0} D^{-1}(\mathbf{k}_0(\tilde{t}))\nabla_{k_\beta}\mathcal{E}_M(\mathbf{k}_0(\tilde{t}))\cdot\exp(i\tilde{\omega}\tilde{t})\exp(\tilde{t})d\tilde{t}=e\tau_S^{-1}\sigma_{\alpha\beta}^{reg}(1,1,T\tau_S,e\mathbf{B},\omega\tau_S,\tau_S\varepsilon_M) \quad (22)$$

where in the above equation, we have used the notation:

$$\frac{\partial f_{0T}(\varepsilon_M(\mathbf{k}))}{\partial\varepsilon}\equiv\frac{\partial}{\partial\varepsilon_M}\left(\frac{1}{1+\exp(\beta\varepsilon_M)}\right)=\frac{\partial}{\partial\mathcal{E}_M}\left(\frac{1}{1+\exp(\beta\mathcal{E}_M/\tau_S)}\right)\equiv\frac{\partial f_{0T\tau_S}(\mathcal{E}_M(\mathbf{k}))}{\partial\mathcal{E}}. \quad (23)$$

This scaling relation will be useful for the numerical calculations in the following sections. In addition, as $\sigma_{\alpha\beta}^{reg}(1,1,T\tau_S,e\mathbf{B},\omega\tau_S,\tau_S\varepsilon_M)$ is a power series in eB, it is impossible to completely disentangle

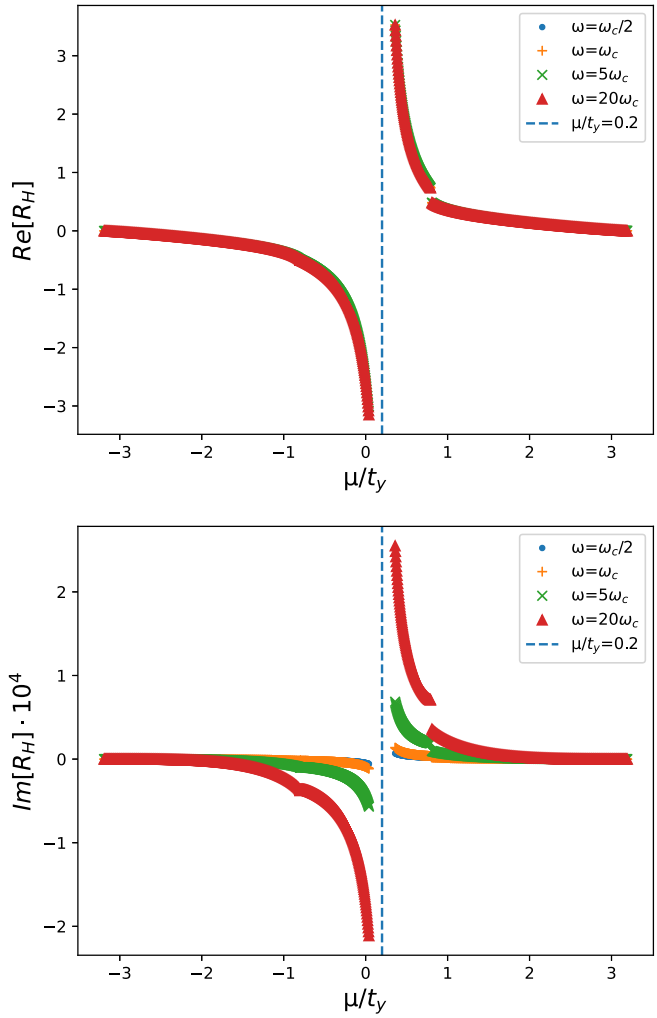

FIG. 1. The real and imaginary part of the Hall number for four different frequencies, B=0.01 and $\omega_c\tau_S = 0.01$ for the example of the rectangular lattice. The Lifshitz transition occurs is at $\mu = 0.25$. The results are valid away form $\mu = 0.25$ where magnetic breakdown phenomena should be taken into account for a full analysis.

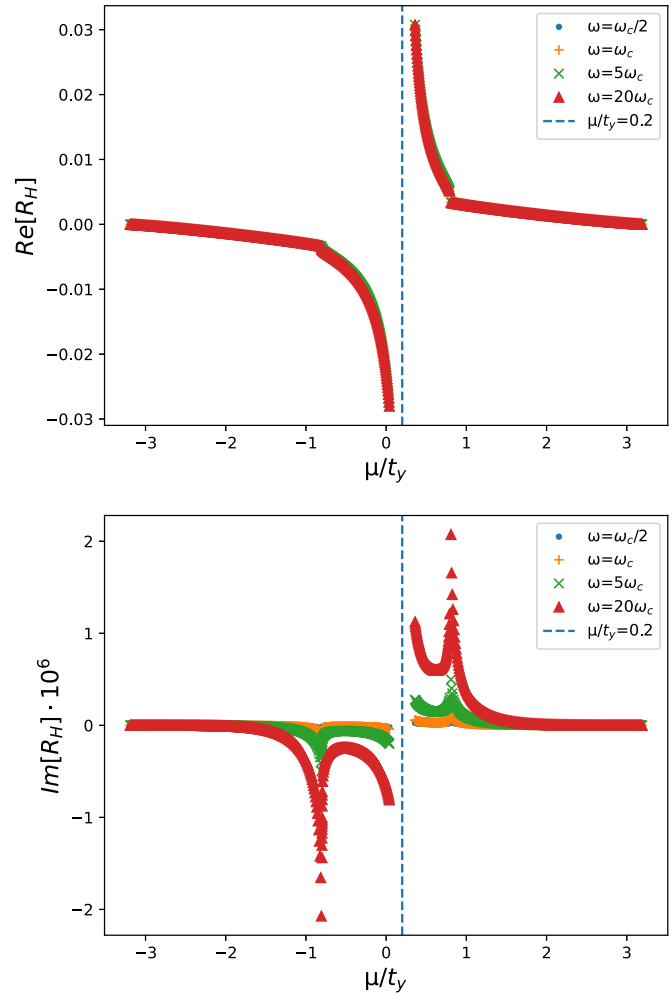

FIG. 2. Same as in Fig. 1 the real and imaginary part of the Hall number for four different frequencies and now for $\omega_c\tau_S = 1$. As before, the results are valid away from the Lifshitz transition.

all the powers of e that enter the expression for the conductivity.

IV. LIFSHITZ TRANSITION OF NECK FORMATION/ COLLAPSE ON RECTANGULAR LATTICE

We use the frequency dependent Chambers formula to calculate the components of the conductivity tensor in the case of an energy dispersion of the form

$$\varepsilon(k) = -2t_x \cos(k_x) - 2t_y \cos(k_y)\ (t_y > t_x). \tag{24}$$

We define $\mu_c = 2(t_y - t_x)$ and $\mu_0 = 2(t_y + t_x)$. For this band we have got the following topologies:

$$\begin{aligned} -\mu_0 < \mu < -\mu_c &\quad \text{electron pockets,} \\ -\mu_c < \mu < \mu_c &\quad \text{open Fermi surface,} \\ \mu_c < \mu < \mu_0 &\quad \text{hole pockets.} \end{aligned} \tag{25}$$

The components of σ for all three cases read (the details of all calculations in this section are left in Appendix C1):

$$\sigma^i_{xx} = \frac{2\sigma_0}{K}\sum_n \frac{[1+i\omega\tau_S]\mathrm{sech}^2\left[\frac{n\pi K'}{2K}\right]\sin^2\left[\frac{n\pi u_i}{2K}\right]}{[1+i\omega\tau_S]^2+[n\omega_c\tau_S]^2}, \tag{26}$$

$$\begin{aligned}\sigma^i_{yy} = {}& \frac{\sigma_0\delta_{i,o}}{K}\frac{1}{1+i\omega\tau_S} \\ &+ \frac{2\sigma_0}{K}\sum_n \frac{[1+i\omega\tau_S]\mathrm{sech}^2\left[\frac{n\pi K'}{2K}\right]\cos^2\left[\frac{n\pi u_i}{2K}\right]}{[1+i\omega\tau_S]^2+[n\omega_c\tau_S]^2},\end{aligned} \tag{27}$$

$$\begin{aligned}\sigma^i_{xy} = {}& (\delta_{i,o}+\delta_{i,e}-\delta_{i,h})\frac{\sigma_0}{K} \\ &\times \sum_n \frac{(n\omega_c\tau_S)\mathrm{sech}^2\left[\frac{n\pi K'}{2K}\right]\sin\left[\frac{n\pi u_i}{K}\right]}{[1+i\omega\tau_S]^2+[n\omega_c\tau_S]^2},\end{aligned} \tag{28}$$

where h stands for hole orbits, e stands for electron orbits and o stands for open orbits. Furthermore, we have defined that $\kappa = \sqrt{\frac{\mu_0^2-\mu^2}{\mu_0^2-\mu_c^2}}$, $\omega_0 = eB\sqrt{4t_xt_y}$, $m_0 = \frac{1}{\sqrt{4t_xt_y}}$, $\sigma_0 = e^2\tau_S\sqrt{4t_xt_y}$, and $K(\kappa)$ is the complete elliptic integral of the first kind. In the case of closed surfaces $K \equiv K(\kappa)$, $K' \equiv K(\sqrt{1-\kappa^2})$. For

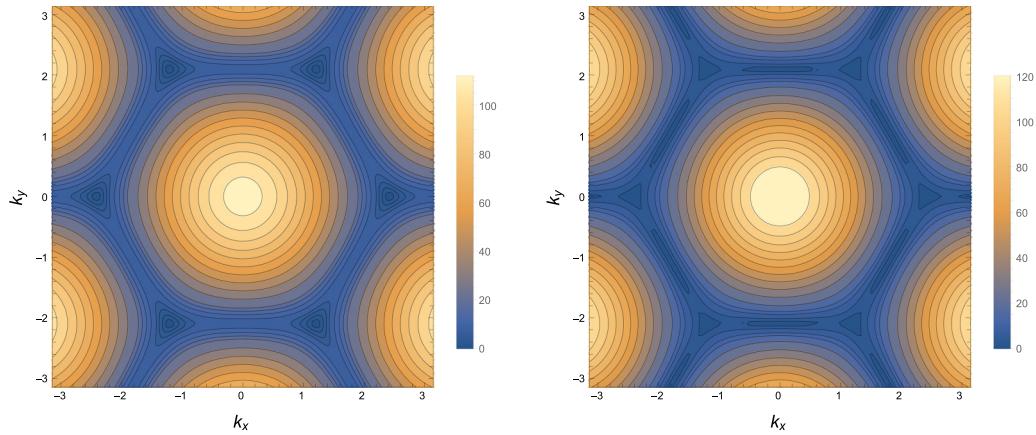

FIG. 3. Dispersion for graphene with third-nearest neighbors for $c/t = 1/4$ where the higher order Van Hove singularity (cusp, on the left) can be visualized at $\mathbf{G} = \frac{2\pi}{3}(0, 1)$. For $c/t = 1/3$ (on the right) it is a nodal point with ill-defined gradient. For the plots we take $t = 30$.

open surfaces we substitute $K(\kappa) \to \frac{1}{\kappa}K(1/\kappa)$ and similarly for K' [56]. In addition

$$\omega_c = \begin{cases} \frac{\pi\omega_0}{2K(\kappa)} & \text{closed orbits} \\ \frac{\pi\kappa\omega_0}{2K(1/\kappa)} & \text{open trajectories} \end{cases}. \tag{29}$$

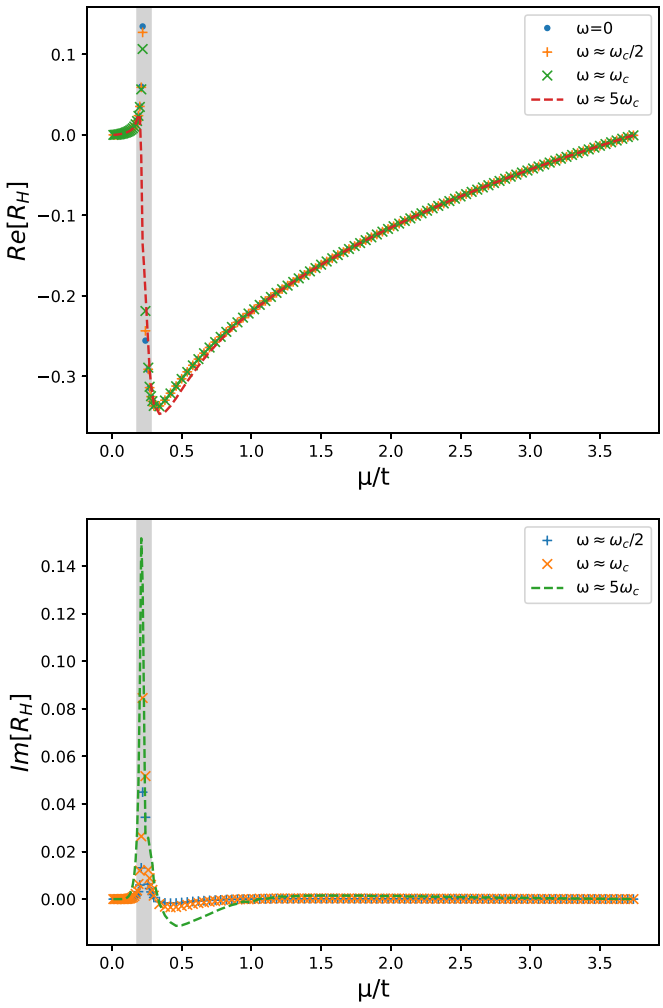

FIG. 4. Real and imaginary part of Hall coefficient for $\omega_c\tau_S = 0.3$.

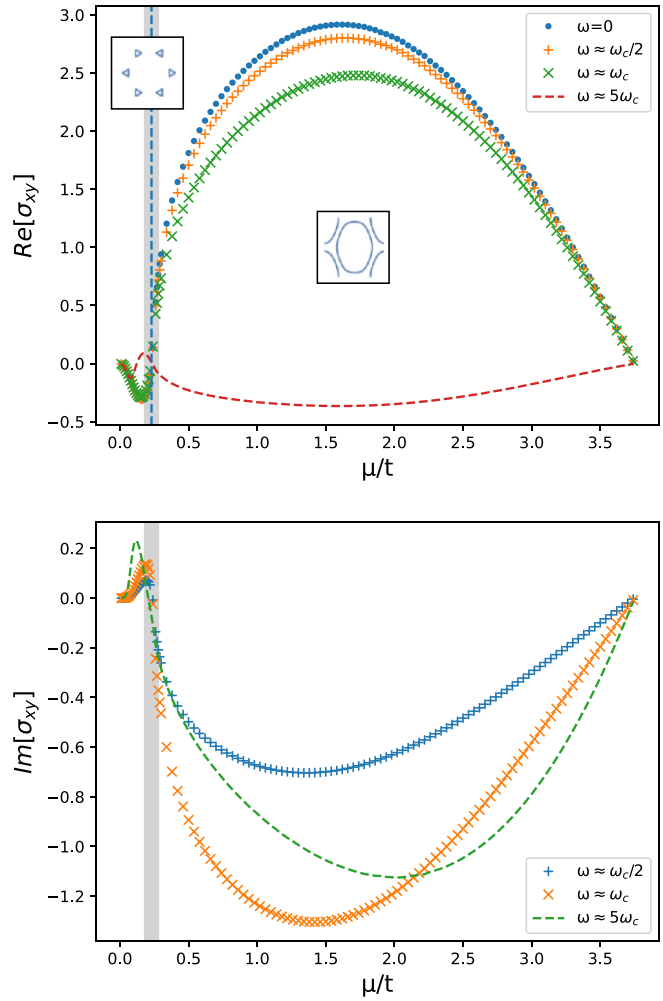

FIG. 5. Real and imaginary part of Hall conductivity for $\omega_c\tau_S = 0.3$ for the simple model of highly doped graphene. On the left figure, the Fermi surfaces in different regimes have been depicted, so the topological transition is evident. The shaded areas, around FSTTs, denote where magnetic breakdown phenomena should be taken into account for a full quantitative analysis.

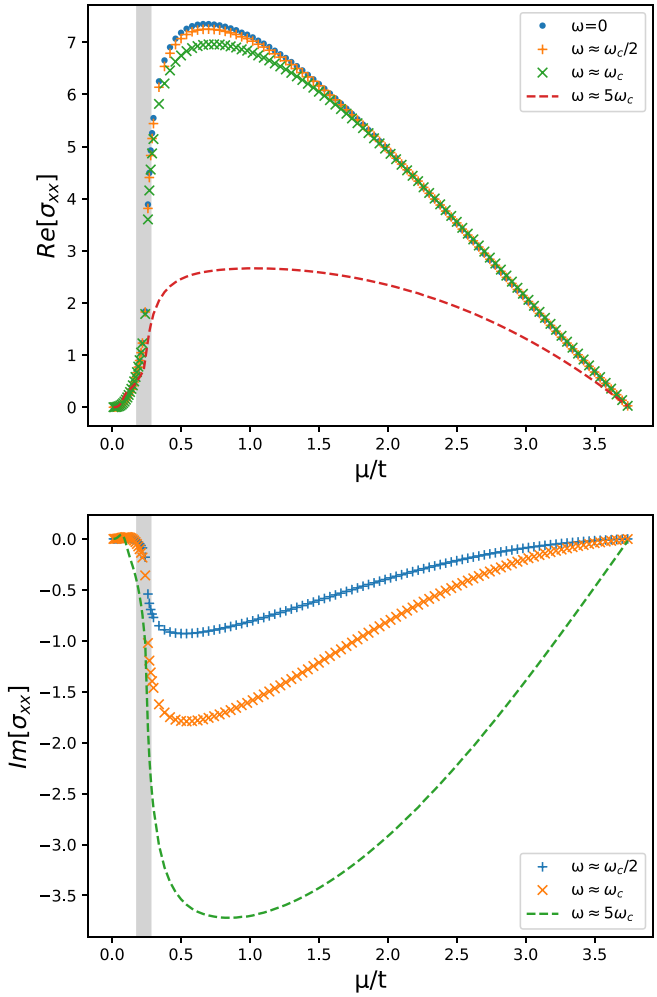

FIG. 6. Real and imaginary part of the conductivity σ_{xx} (which is the same as σ_{yy}) for $\omega_c\tau_S = 0.3$.

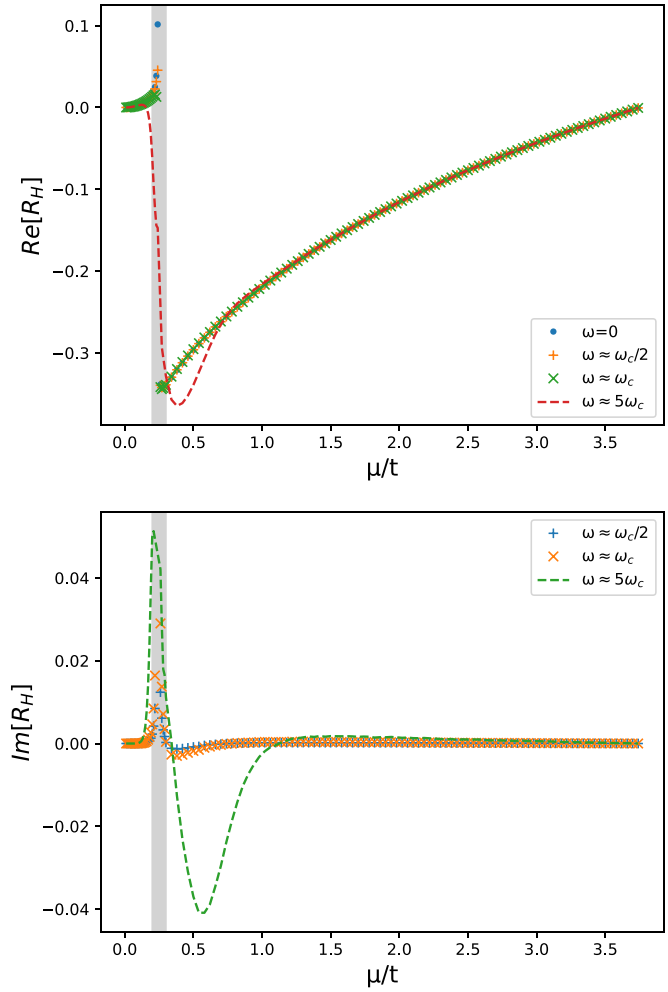

FIG. 7. Real and imaginary part of Hall coefficient for $\omega_c\tau_S = 1$.

Finally u_i and u_o are defined via Jacobean elliptic functions:

$$\mathrm{sn}(u_e, \kappa) = \sqrt{\frac{\mu_0 - \mu_c}{\mu_0 - \mu}}, \tag{30}$$

$$\mathrm{sn}(u_h, \kappa) = \sqrt{\frac{\mu_0 - \mu_c}{\mu_0 + \mu}}, \tag{31}$$

$$\mathrm{sn}(\kappa u_o, 1/\kappa) = \sqrt{\frac{\mu_0 + \mu}{\mu_0 + \mu_c}}. \tag{32}$$

For closed Fermi surfaces the sums are over positive odd integers while for open surfaces the sums are over positive even integers.

The calculation of the Hall number for both high and low magnetic fields leads to expressions that are independent of the frequency and similar to the ones calculated in [56]. For completeness we present the formulas in the Appendix C1. In Figs. 1 and 2 we present the results for two limiting values of $\omega_c\tau_S = 0.01 \ll 1$ and for ≈ 1. For each of these values several different frequencies have been chosen. The magnetic field is $B = 0.01$ in units of $hc/(a^2e)$ where a is the lattice constant (for simplicity we work with $a = h = c = 1$). Consistently with the fact that at $\mu/t_y = 0.25$, there is a regular (logarithmic) Van Hove singularity (in the language of Lifshitz transitions is classified as a neck formation/collapse), the real part of the Hall coefficient changes sign from electron to hole-like. At values of μ/t_y close to ± 1 the discontinuities signal the change from closed pockets to open Fermi surface. The real part does not show any significant frequency dependence. On the contrary, the imaginary part displays a strong frequency dependence with all features (change of sign at the Lifshitz transition and discontinuity at close-open Fermi surface transition) becoming more pronounced with increasing ω. Away from these special values of μ/t_y, the imaginary part of the Hall number is practically zero, reflecting that the dispersion relation is parabolic. Close to the Lifshitz transition quantum tunneling must be taken into account for full quantitative analysis [43,44].

V. SUPERMETAL: A SIMPLE MODEL FOR HIGHLY DOPED GRAPHENE

A. A relevant tight binding model

We will consider a Hamiltonian on hexagonal lattice, which is relevant to recent studies of graphene that showed the emergence of a higher order Van Hove singularity [21,22].

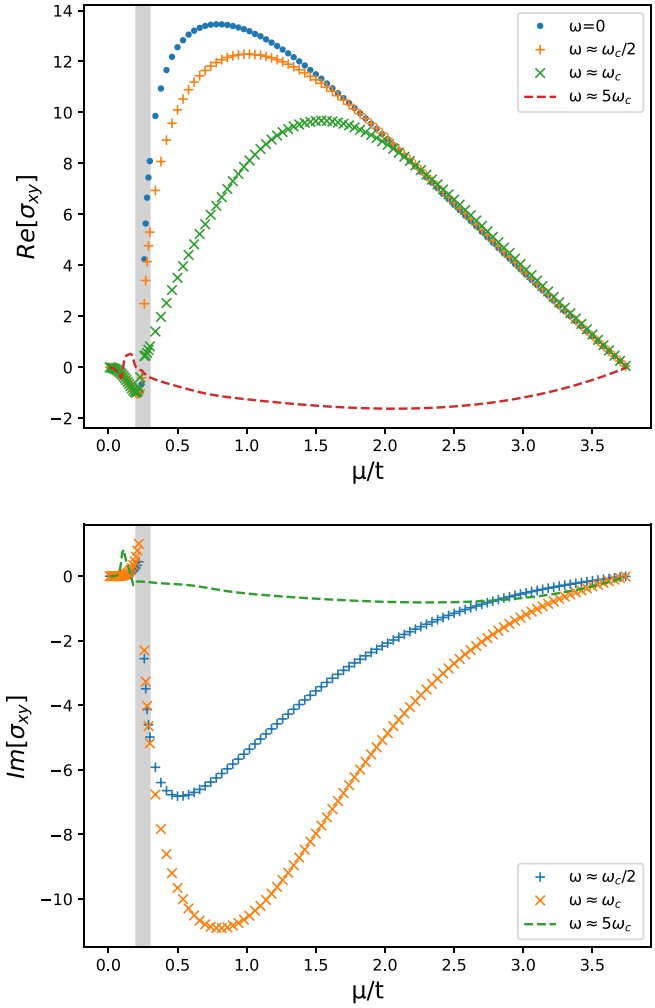

FIG. 8. Real and imaginary part of Hall conductivity for $\omega_c\tau_S = 1$.

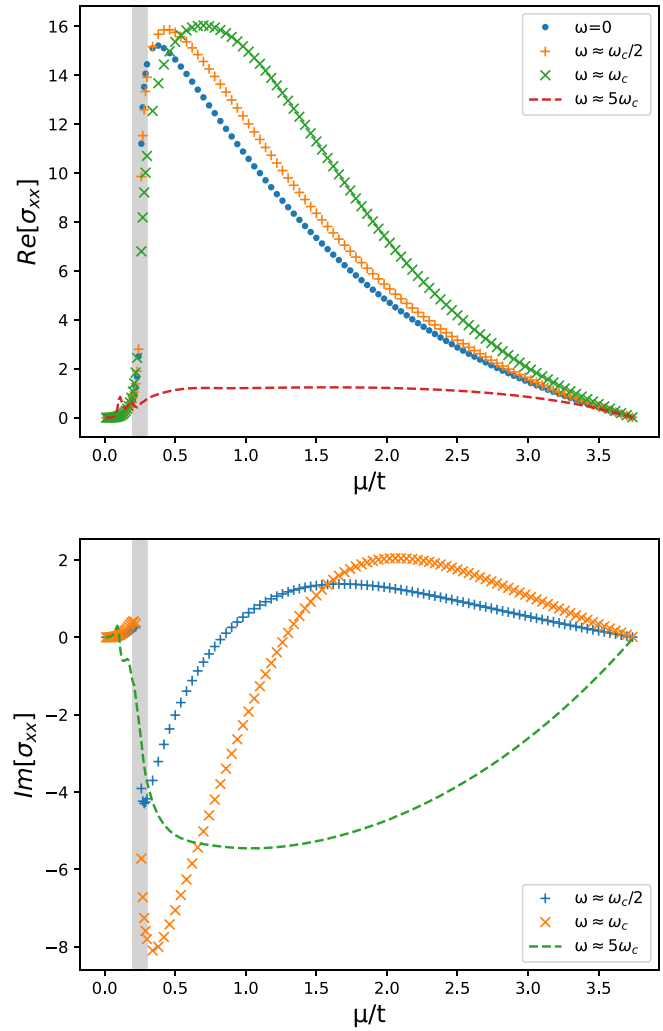

FIG. 9. Real and imaginary part of the conductivity σ_{xx} (same as σ_{yy}) for $\omega_c\tau_S = 1$.

By considering third-nearest-neighbors tunneling the simple Hamiltonian that generates higher order Van Hove singularities, as a consequence of FSTTs, reads

$$H = \begin{pmatrix} 0 & f(\mathbf{k}) \\ f^*(\mathbf{k}) & 0 \end{pmatrix} \tag{33}$$

where

$$f(\mathbf{k}) = -t[e^{-ik_y} + e^{\frac{i}{2}(\sqrt{3}k_x+k_y)} + e^{\frac{i}{2}(-\sqrt{3}k_x+k_y)}] - c[e^{i2k_y} + e^{-i(\sqrt{3}k_x+k_y)} + e^{-i(-\sqrt{3}k_x+k_y)}] \tag{34}$$

and energy dispersion $E_\pm(k) = \pm\sqrt{f^*(\mathbf{k})f(\mathbf{k})}$.

This leads to a higher order Van Hove saddle in both $E_\pm(\mathbf{k})$ at wave vector $\mathbf{G} = \frac{2\pi}{3}(0, 1)$ (for lattice constant $a = 1$) for $c = \frac{t}{4}$ while for $c = \frac{t}{3}$ it is a nodal point with closure of gap and ill defined gradient. It is rather instructive to present the contour plots of E_+ for both cases in Fig. 3. The higher order saddle for $c = \frac{t}{4}$ is a cusp at $\mathbf{G} = \frac{2\pi}{3}(0, 1)$, based on the catastrophe theory classification [5,20].

B. Numerical results

The numerical results for the Hall coefficient as well as the conductivity components are presented in Figs. 4–9. From the scaling formula Eq. (22) $T\tau_S \to 0$ and we take $eB \to 0.01$ for the calculations. In this case ω_c is defined as $\omega_c = \frac{eB}{m^{*c}}$ with the effective mass $m^* \propto t^{-1}$. We have chosen again two values of $\omega_c\tau_S$ (0.3 and 1) and for each one three frequencies ω for the time-dependent electric field. For $c/t = 1/4$, the higher order Van Hove singularity is at $\mu/t = 0.25$. This explains the sharp features of the conductivities and the change of sign of the Hall coefficient at that value. In Fig. 5(a) the Fermi surface topology is depicted across both sides of the discontinuous behavior. The maximum of the real part of the conductivity takes place when the area of the Fermi surface is largest. The frequency dependence is pronounced in the imaginary part of the Hall coefficient R_H and around the value of $\mu/t = 0.25$. Away from $\mu/t = 0.25$ the imaginary part of R_H is zero, while for the real part of R_H the behavior is linear in μ/t. This result is very well explained by the fact that away from the FSTT, the dispersion relation is very well approximated by a parabolic one with precisely this behavior as the imaginary part of ρ_{xy} is 0 and for the real part $\rho_{xy} \propto B/(ne)$, where n is the density of electrons, which is linear in μ. As a result R_H exhibits that behavior for $\mu/t > 1$. As the frequency is increased the

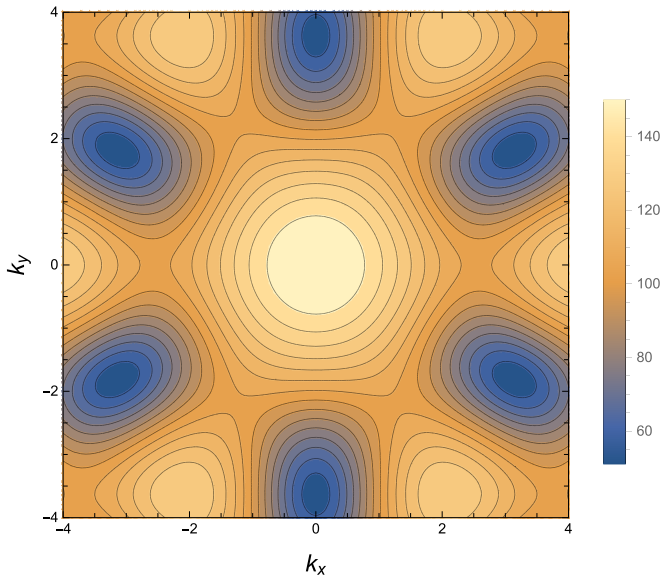

FIG. 10. Energy contours of the Haldane model, the parameters we use are mentioned in the text.

region where there is appreciable effect of the singularity is larger.

VI. HALL CONDUCTIVITY OF THE HALDANE MODEL

We consider the Haldane Hamiltonian on a honeycomb lattice with $H(\theta) = d_0(\theta) + \mathbf{d}(\theta)\cdot\sigma$ where

$$d_0(\theta) = -2t_2[\cos\theta_1 + \cos\theta_2 + \cos(\theta_1+\theta_2)]\cos\phi,$$
$$d_x(\theta) = -t_1(1+\cos\theta_1+\cos\theta_2),$$

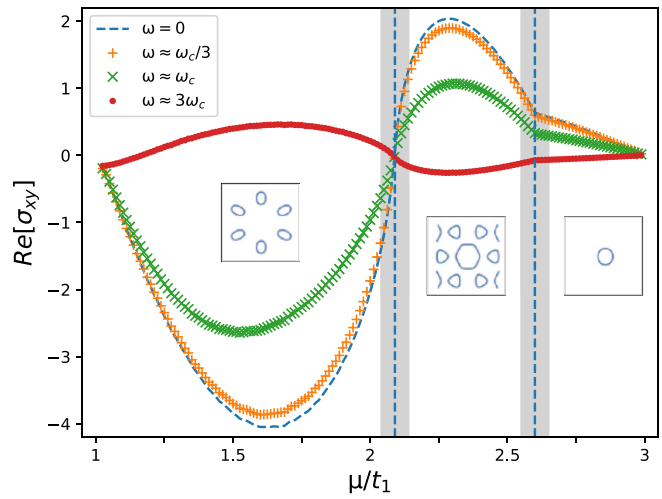

FIG. 11. The real part of the Hall conductivity. In the various parts of the curve, the Fermi surface topology is shown. All conductivities are in units of $e^2\tau_S$. For the second term of Eq. (18), which we call "regular" term, we use the scaling relation: $\sigma^{reg}_{\alpha\beta}(e,\tau_S,T,\mathbf{B},\omega,\varepsilon_M) = e\tau_S^{-1}\sigma^{reg}_{\alpha\beta}(1,1,T\tau_S,e\mathbf{B},\omega\tau_S,\tau_S\varepsilon_M)$. As before, the shaded areas denote the places where magnetic breakdown phenomena should be taken into account for a full quantitative analysis.

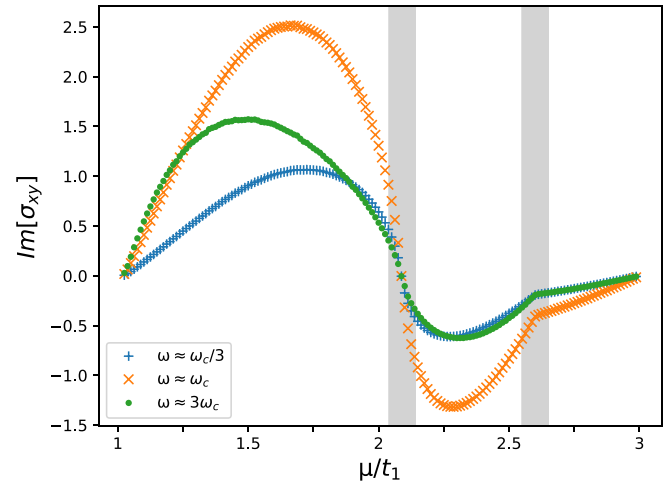

FIG. 12. Imaginary part of the Hall conductivity. This comes solely from the second term of Eq. (18).

$$d_y(\theta) = t_1(\sin\theta_1 - \sin\theta_2),$$
$$d_z(\theta) = m - 2t_2[\sin\theta_1 + \sin\theta_2 - \sin(\theta_1+\theta_2)]\sin\phi,$$

and σ denotes the Pauli matrices. The energy eigenvalues are given by $E_\pm = d_0 \pm |d_1|$. For simplicity, we choose $\phi = \pi/2$, $m = 0$ and consider E_+ for $t_1 = 50$ and $t_2 = 25$ with a nontrivial Chern number of –1. The energy contours of the model is presented in Fig. 10. We numerically calculate the Hall conductivity and present the results in Figs. 11–14. The real part of the Hall conductivity shows different behavior in different regimes of the chemical potential reflecting the different Fermi surface topology. This topology of the Fermi surface is shown in the insets of Fig. 2, in each segment where the behavior is different. In the value of the total Hall conductivity a constant $-\frac{1}{2\pi}$ has been added in Fig. 2, due to the contribution of the lower band. The results are for $\omega_c\tau_S = 0.3$, where $\omega_c = \frac{eB}{m^*c}$ and the effective mass $m^* \propto {t_1}^{-1}$ and $eB = 0.01$. The contributions from the different terms of

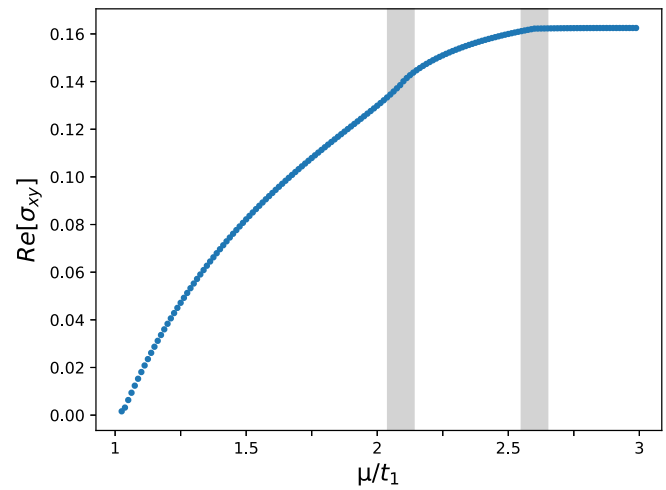

FIG. 13. First term of Hall conductivity as given by Eq. (18). It has no frequency dependence. The range of the values is from 0 to $\pi/2$, indicating that, for $e = 1$, the Chern number is -1.

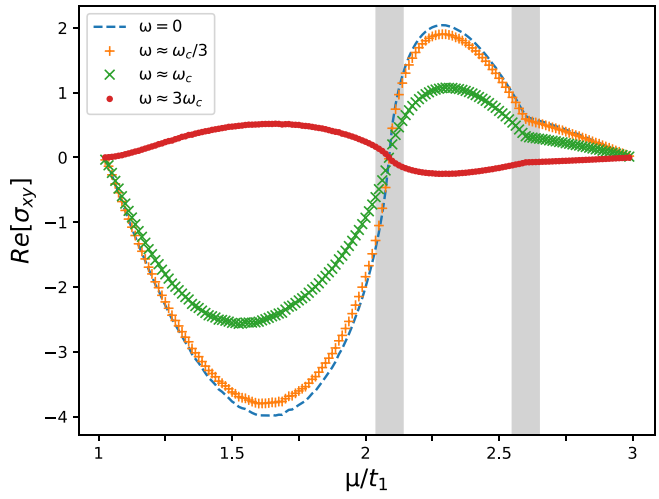

FIG. 14. The real part of the second term of Hall conductivity.

Eq. (19) are presented separately and the significant role of the second term of Eq. (19) is clearly demonstrated.

VII. CONCLUSIONS

In this paper a generalization of the celebrated Chambers formula has been introduced, relevant to time-dependent electric fields and bands with Berry curvature. The nonlinear conductivity, to order E^2 in the electric field has been also computed within the leading order equations of motion method. These general formulas have been used to study a number of examples. In particular, we studied bands where by changing the chemical potential a range of FSTTs become available. These FSTTs lead to Van Hove singularities at the Fermi surface where the high density of states but our paper is valid away from the regions close to the topological transitions to avoid considering quantum Hall or out-of-equilibrium effects. Due to the change of the Fermi surface from hole like to electron like there is a jump in the Hall coefficient of the material at the Fermi surface topological transition, while a wealth of different features and signatures appear both in real and imaginary parts of the Hall coefficient and conductivities, especially pronounced at higher frequencies. Different types of FSTTs provide their signatures on the conductivities. Furthermore, the Hall conductivity of the Haldane model has been studied.

The main assumption of the general part of our paper is that the system is a Fermi liquid and the effects of the interactions can be included in the lifetime and the effective mass. There is recent seminal paper that takes into account strong interactions [57] and presents a formula that does not require the existence of quasiparticles. We leave as a future work how to bridge the two approaches. Given the enormous interest in the field, we believe that this paper will stimulate significant future activity associated with applications of the extended, formally exact Chambers formulas presented here. This paper is based on simplified semiclassical equations of motion that are commonly used but are only strictly valid to leading order in the electric and magnetic fields. As it has been already emphasized, close to Van Hove singularities, magnetic breakdown effects (quantum tunneling), must be taken into account [43,44]. These will be considered elsewhere.

ACKNOWLEDGMENTS

We would like to thank Claudio Chamon, Anirudh Chandrasekaran, Mark Greenaway, and Xenophon Zotos for useful discussions. The work has been supported by the EPSRC Grants No. EP/P002811/1 and No. EP/T034351/1 (J.J.B.). D.V.E. was supported by the RSF-DFG Grant No. 405940956.

APPENDIX A: CHAMBERS FORMULA

1. Boltzmann Equation

Following the Chambers original paper [25] we write the current as

$$J_\alpha(t) = -e\int \frac{d^3k}{(2\pi)^3}\frac{d\mathbf{r}_\alpha}{dt}(\mathbf{k})f(\mathbf{k},t) \tag{A1}$$

with $f(\mathbf{k},t)$ being the solution to the Boltzmann equation:

$$\frac{\partial f(\mathbf{k},t)}{\partial t} + \frac{d\mathbf{k}}{dt}\frac{\partial f(\mathbf{k},t)}{\partial \mathbf{k}} = \frac{1}{\tau_S(\mathbf{k})}\{f_0[\varepsilon_M(\mathbf{k})] - f(\mathbf{k},t)\} \tag{A2}$$

with

$$\frac{d\mathbf{k}}{dt} = -e[\nabla_{\mathbf{k}}\varepsilon(\mathbf{k}) \times \mathbf{B} + \mathbf{E}(t)], \tag{A3}$$

$$\frac{d\mathbf{r}}{dt} = \nabla_{\mathbf{k}}\varepsilon(\mathbf{k}). \tag{A4}$$

The solution as is well known, is given by

$$f(\mathbf{k},t) = \int_{-\infty}^{t} \frac{f_0\{\varepsilon[\mathbf{k}(t')]\}}{\tau_S(\mathbf{k}(t'))}\exp\left(-\int_{t'}^{t}\frac{ds}{\tau_S(\mathbf{k}(s))}\right)dt'. \tag{A5}$$

2. Momentum as a function of time

In the limit where $\mathbf{E}(t)$ is small the second term on the right-hand side of Eq. (A3) may be viewed as a perturbation. In that spirit let us denote by $\mathbf{k}_0(t)$ the solution to the equation:

$$\frac{d\mathbf{k_0}(t)}{dt} = -e\nabla_{\mathbf{k}}\varepsilon(\mathbf{k}_0(t)) \times \mathbf{B}. \tag{A6}$$

If we write: $\mathbf{E}(t) = \lambda\mathbf{E}(t)$ with $\lambda = 1$, then the solution to Eq. (A3) can be written as

$$\mathbf{k}(t) = \mathbf{k}_0(t) + \lambda\mathbf{k}_1(t) + \lambda^2\mathbf{k}_2(t) + \cdots \tag{A7}$$

with $\mathbf{k}_1(t_0) = \mathbf{k}_2(t_0) = \mathbf{k}_3(t_0) = \cdots = 0$. Then, to order λ we obtain

$$\frac{d\mathbf{k}_1(t)}{dt} = -e\left[\sum_\alpha k_{1\alpha}(t)\frac{\partial}{\partial k_\alpha}\nabla_{\mathbf{k}}\varepsilon(\mathbf{k}_0(t))\right] \times \mathbf{B} - e\mathbf{E}(t). \tag{A8}$$

In addition

$$\begin{aligned}\frac{d\varepsilon(\mathbf{k}(t))}{dt} &= \nabla_{\mathbf{k}}\varepsilon(\mathbf{k}(t)) \cdot \frac{d\mathbf{k}}{dt} \\ &= -e\nabla_{\mathbf{k}}\varepsilon(\mathbf{k}) \cdot [\nabla_{\mathbf{k}}\varepsilon(\mathbf{k}) \times \mathbf{B} + \mathbf{E}(t)] \\ &= -e\nabla_{\mathbf{k}}\varepsilon(\mathbf{k}(t)) \cdot \mathbf{E}(t).\end{aligned} \tag{A9}$$

We can now similarly expand in powers of λ:

$$\varepsilon_M(t) = \varepsilon_0(t) + \lambda\varepsilon_1(t) + \lambda^2\varepsilon_2(t) + \cdots \tag{A10}$$

with $\varepsilon_1(t_0) = \varepsilon_2(t_0) = \varepsilon_3(t_0) = \cdots = 0$. To order λ for $t > t_0$:

$$\varepsilon_1(t) = e\int_{t_0}^{t} \nabla_{\mathbf{k}}\varepsilon(\mathbf{k}_0(s))\cdot\mathbf{E}(s)ds \tag{A11}$$

and

$$\varepsilon_2(t) = e\sum_{\alpha\beta}\int_{t_0}^{t} E_\beta(s)k_{1\alpha}(s)\frac{\partial^2}{\partial k_\alpha \partial k_\beta}\varepsilon(\mathbf{k}_0(s))ds. \tag{A12}$$

3. Calculation of the current in linear response in 3D

We first note the identity:

$$\int_{-\infty}^{t}\frac{dt'}{\tau_S(\mathbf{k}(t'))}\exp\left(-\int_{t'}^{t}\frac{ds}{\tau_S(\mathbf{k}(s))}\right) = 1, \tag{A13}$$

therefore there is no need to expand the term $\int_{-\infty}^{t}\frac{dt'}{\tau_S(\mathbf{k}(t'))}\exp(-\int_{t'}^{t}\frac{ds}{\tau_S(\mathbf{k}(s))})$ in Eq. (A5). As a result we obtain:

$$f(\mathbf{k},t) = f_0(\varepsilon(\mathbf{k}_0(t))) + \frac{\partial f_0(\varepsilon(\mathbf{k}_0(t)))}{\partial\varepsilon}\int_{-\infty}^{t}dt'\frac{\varepsilon_1(t')}{\tau_S(\mathbf{k}_0(t'))}\eta(t;t').$$

Noticing that the current is written as

$$J_\alpha(t) = \frac{\partial f_0\{\varepsilon[\mathbf{k}_0(t)]\}}{\partial\varepsilon}\int_{-\infty}^{t}\frac{\varepsilon_1(t')}{\tau_S(\mathbf{k}_0(t'))}\eta(t;t')dt' \tag{A14}$$

to obtain the result to first order in the electric field (linear response), all terms $\sim E^2$ are neglected and a term is dropped due to the relation: $-e\int\frac{d^3k}{(2\pi)^3}\nabla_{\mathbf{k}}\varepsilon(\mathbf{k})f_0\{\varepsilon[\mathbf{k}_0(t)]\} = 0$ as there is no current without an electric field. Then

$$J_\alpha(t) = -e\int\frac{d^3k}{(2\pi)^3}\nabla_{k_\alpha}\varepsilon(\mathbf{k})\cdot\left[\frac{\partial f_0\{\varepsilon[\mathbf{k}_0(t)]\}}{\partial\varepsilon}\int_{-\infty}^{t}dt'\frac{\varepsilon_1(t')}{\tau_S(\mathbf{k}_0(t'))}\eta(t;t')\right] \tag{A15}$$

The first term in the bracket in Eq. (A15) is what Chambers calculated and it is given by [25,26], we can integrate it by parts using $\frac{d}{dt}\varepsilon_1(t) = -e\nabla_{\mathbf{k}}\varepsilon(\mathbf{k}_0(t))\cdot\mathbf{E}(t)$ to obtain the final expression:

$$J_\alpha(t) = -e^2\int\frac{d^3k}{(2\pi)^3}\nabla_{k_\alpha}\varepsilon(\mathbf{k})\frac{\partial f_0(\varepsilon(\mathbf{k}))}{\partial\varepsilon}\int_{-\infty}^{t}dt'\nabla_{\mathbf{k}}\varepsilon(\mathbf{k}_0(t'))\cdot\mathbf{E}(t)\eta(t;t'). \tag{A16}$$

4. Calculation of nonlinear current to order $\mathbf{E}^2$

To proceed with the next order term, we note that

$$\begin{aligned}
f(\mathbf{k},t) &\simeq \int_{-\infty}^{t}\frac{f_0(([\varepsilon_0+\varepsilon_1+\varepsilon_2](t')))}{\tau_S([\mathbf{k}_0+\mathbf{k}_1+\mathbf{k}_2](t'))}\exp\left(-\int_{t'}^{t}\frac{ds}{\tau_S([\mathbf{k}_0+\mathbf{k}_1+\mathbf{k}_2](s))}\right)dt' \\
&\cong \int_{-\infty}^{t}\frac{f_0\{\varepsilon[\mathbf{k}_0(t)]\}}{\tau_S(\mathbf{k}_0(t'))}\eta(t;t')dt' + \frac{\partial f_0\{\varepsilon[\mathbf{k}_0(t)]\}}{\partial\varepsilon}\int_{-\infty}^{t}\frac{\varepsilon_1(t')+\varepsilon_2(t')}{\tau_S(\mathbf{k}_0(t'))}\eta(t;t')dt' \\
&+ \frac{1}{2}\frac{\partial^2 f_0\{\varepsilon[\mathbf{k}_0(t)]\}}{\partial\varepsilon^2}\int_{-\infty}^{t}\frac{\varepsilon_1^2(t')}{\tau_S(\mathbf{k}_0(t'))}\eta(t;t')dt' - \frac{\partial f_0\{\varepsilon[\mathbf{k}_0(t)]\}}{\partial\varepsilon}\int_{-\infty}^{t}\frac{\varepsilon_1(t)}{\tau_S(\mathbf{k}_0(t'))}\frac{\nabla_{\mathbf{k}}\tau_S(\mathbf{k}_0(t'))\cdot\mathbf{k}_1(t')}{\tau_S(\mathbf{k}_0(t))}\eta(t;t')dt' \\
&+ \frac{\partial f_0\{\varepsilon[\mathbf{k}_0(t)]\}}{\partial\varepsilon}\int_{-\infty}^{t}\frac{\varepsilon_1(t)}{\tau_S(\mathbf{k}_0(t))}\eta(t;t')\int_{t'}^{t}\frac{\nabla_{\mathbf{k}}\tau_S(\mathbf{k}_0(l))\mathbf{k}_1(l)}{\tau_S^2(\mathbf{k}_0(l))}dldt',
\end{aligned} \tag{A17}$$

where Eq. (A13) has been used. Integrating the above expression by parts and using the formula for the current:

$$\begin{aligned}
J_\alpha^{(2)}(t) &= -e^2\int\frac{d^3k}{(2\pi)^3}\nabla_{k_\alpha}\varepsilon(\mathbf{k})\frac{\partial f_0(\varepsilon(\mathbf{k}))}{\partial\varepsilon}\int_{-\infty}^{t}dt'\nabla_{\mathbf{k}}\varepsilon(\mathbf{k}_0(t'))\cdot\mathbf{E}(t)\eta(t;t') \\
&- e\int\frac{d^3k}{(2\pi)^3}\nabla_{k_\alpha}\varepsilon(\mathbf{k})\frac{\partial f_0(\varepsilon(\mathbf{k}))}{\partial\varepsilon}\int_{-\infty}^{t}dt'\frac{\varepsilon_2(t')}{\tau_S(\mathbf{k}_0(t'))}\eta(t;t') \\
&- \frac{1}{2}e\int\frac{d^3k}{(2\pi)^3}\nabla_{k_\alpha}\varepsilon(\mathbf{k})\frac{\partial^2 f_0(\varepsilon(\mathbf{k}))}{\partial\varepsilon^2}\int_{-\infty}^{t}dt'\frac{\varepsilon_1^2(t')}{\tau_S(\mathbf{k}_0(t'))}\eta(t;t') \\
&- e^2\int\frac{d^3k}{(2\pi)^3}\nabla_{k_\alpha}\varepsilon(\mathbf{k})\frac{\partial f_0(\varepsilon(\mathbf{k}))}{\partial\varepsilon}\int_{-\infty}^{t}dt'\nabla_{\mathbf{k}}\varepsilon(\mathbf{k}_0(t'))\cdot\mathbf{E}(t')\eta(t;t')\int_{t'}^{t}\frac{\nabla_{\mathbf{k}}\tau_S(\mathbf{k}_0(l))\cdot\mathbf{k}_1(l)}{\tau_S^2(\mathbf{k}_0(l))}dl
\end{aligned} \tag{A18}$$

finally, after another integration by parts, we obtain the expression of the nonlinear current:

$$\begin{aligned}
J_\alpha^{(2)}(t) &= -e^2\int\frac{d^3k}{(2\pi)^3}\nabla_{k_\alpha}\varepsilon(\mathbf{k})\frac{\partial f_0(\varepsilon(\mathbf{k}))}{\partial\varepsilon}\int_{-\infty}^{t}dt'\nabla_{\mathbf{k}}\varepsilon(\mathbf{k}_0(t'))\cdot\mathbf{E}(t)\eta(t;t') \\
&- e^2\int\frac{d^3k}{(2\pi)^3}\nabla_{k_\alpha}\varepsilon(\mathbf{k})\frac{\partial f_0(\varepsilon(\mathbf{k}))}{\partial\varepsilon}\int_{-\infty}^{t}dt'\sum_{\beta\gamma}E_\beta(t')k_{1\gamma}(t')\frac{\partial^2}{\partial k_\gamma\partial k_\beta}\varepsilon(\mathbf{k}_0(t'))\eta(t;t')
\end{aligned}$$

$$- e^3 \frac{\partial^2 f_0\{\varepsilon[\mathbf{k}_0(t)]\}}{\partial \varepsilon^2} \int_{-\infty}^{t} dt' \nabla_{\mathbf{k}} \varepsilon(\mathbf{k}_0(t')) \cdot \mathbf{E}(t') \eta(t;t') \int_{t'}^{t} \nabla_{\mathbf{k}} \varepsilon(\mathbf{k}_0(l)) \cdot \mathbf{E}(l) dl$$

$$- e^2 \int \frac{d^3k}{(2\pi)^3} \nabla_{k_\alpha} \varepsilon(\mathbf{k}) \frac{\partial f_0(\varepsilon(\mathbf{k}))}{\partial \varepsilon} \int_{-\infty}^{t} dt' \nabla_{\mathbf{k}} \varepsilon(\mathbf{k}_0(t')) \cdot \mathbf{E}(t') \eta(t;t') \int_{t'}^{t} \frac{\nabla_{\mathbf{k}} \tau_S(\mathbf{k}_0(l)) \cdot \mathbf{k}_1(l)}{\tau_S^2(\mathbf{k}_0(l))} dl \tag{A19}$$

APPENDIX B: INCLUSION OF BERRY CURVATURE

1. Calculation of the current in 3D in linear response

The distribution function is written as

$$f(\mathbf{k},t) \simeq \int_{-\infty}^{t} \frac{dt}{\tau_S(\mathbf{k}_0(t))} f_0(\varepsilon_M(\mathbf{k}(t))) \eta(t;t') + \frac{\partial f_0(\varepsilon_M(\mathbf{k}_0(t)))}{\partial \varepsilon} \int_{-\infty}^{t} dt' \frac{\varepsilon_1(t')}{\tau_S(\mathbf{k}_0(t'))} \eta(t;t'). \tag{B1}$$

Substituting Eq. (B1) into Eq. (9) we get that the current is:

$$\begin{aligned} J_\alpha(t) &= -e \int \frac{d^3k}{(2\pi)^3} \frac{dr_\alpha}{dt} D(\mathbf{k}) f(\mathbf{k},t) \\ &= -e \int \frac{d^3k}{(2\pi)^3} D(\mathbf{k}) [u_{\mathbf{0}\alpha}(\mathbf{k}) + D^{-1}(\mathbf{k}) [e\mathbf{E}(t) \times \mathbf{\Omega}(k)]_\alpha] \\ &\quad \times \left[f_0(\varepsilon_M(\mathbf{k}(t))) \int_{-\infty}^{t} \frac{dt'}{\tau_S(\mathbf{k}_0(t'))} \eta(t;t') + \frac{\partial f_0(\varepsilon_M(\mathbf{k}_0(t)))}{\partial \varepsilon} \int_{-\infty}^{t} dt' \frac{\varepsilon_1(t')}{\tau_S(\mathbf{k}_0(t'))} \eta(t;t') \right] \end{aligned}$$

Following similar steps as before to obtain the linear response, we get Eq. (15) of the main text.

2. Calculation of nonlinear current to order E^2 in 3D

In this case, the distribution function reads:

$$\begin{aligned} f(\mathbf{k},t) \cong & \int_{-\infty}^{t} \frac{f_0(\varepsilon(\mathbf{k}_0(t)))}{\tau_S(\mathbf{k}_0(t'))} \eta(t;t') dt' + \frac{\partial f_0(\varepsilon(\mathbf{k}_0(t)))}{\partial \varepsilon} \int_{-\infty}^{t} \frac{\varepsilon_1(t') + \varepsilon_2(t')}{\tau_S(\mathbf{k}_0(t'))} \eta(t;t') dt' \\ & + \frac{1}{2} \frac{\partial^2 f_0(\varepsilon(\mathbf{k}_0(t)))}{\partial \varepsilon^2} \int_{-\infty}^{t} \frac{\varepsilon_1^2(t')}{\tau_S(\mathbf{k}_0(t'))} \eta(t;t') dt' \\ & - \frac{\partial f_0(\varepsilon(\mathbf{k}_0(t)))}{\partial \varepsilon} \int_{-\infty}^{t} dt' \frac{d\varepsilon_1(t')}{dt} \eta(t;t') \int_{t'}^{t} \frac{\nabla_{\mathbf{k}} \tau_S(\mathbf{k}_0(l)) \cdot \mathbf{k}_1(l)}{\tau_S^2(\mathbf{k}_0(l))} dl. \end{aligned} \tag{B2}$$

Then, we obtain for the current:

$$\begin{aligned} J_\alpha(t) = & -e \int \frac{d^3k}{(2\pi)^3} D(\mathbf{k}) [u_{\mathbf{0}\alpha}(\mathbf{k}) + D^{-1}(\mathbf{k}) e[\mathbf{E}(t) \times \mathbf{\Omega}(\mathbf{k})]_\alpha] \\ & \times \left[\int_{-\infty}^{t} dt' \frac{f_0\{\varepsilon[\mathbf{k}_0(t)]\}}{\tau_S(\mathbf{k}_0(t'))} \exp\left(- \int_{t'}^{t} \frac{ds}{\tau_S(\mathbf{k}_0(s))} \right) + \frac{\partial f_0\{\varepsilon[\mathbf{k}_0(t)]\}}{\partial \varepsilon} \int_{-\infty}^{t} dt' \frac{\varepsilon_1(t') + \varepsilon_2(t')}{\tau_S(\mathbf{k}_0(t'))} \eta(t;t') \right. \\ & + \frac{1}{2} \frac{\partial^2 f_0\{\varepsilon[\mathbf{k}_0(t)]\}}{\partial \varepsilon^2} \int_{-\infty}^{t} \frac{\varepsilon_1^2(t)}{\tau_S(\mathbf{k}_0(t))} \eta(t;t') dt' - \frac{\partial f_0\{\varepsilon[\mathbf{k}_0(t)]\}}{\partial \varepsilon} \int_{-\infty}^{t} dt' \frac{d\varepsilon_1(t')}{dt} \eta(t;t') \int_{t'}^{t} \frac{\nabla_{\mathbf{k}} \tau_S(\mathbf{k}_0(l)) \cdot \mathbf{k}_1(l)}{\tau_S^2(\mathbf{k}_0(l))} dl \Bigg]. \end{aligned}$$

Focusing on terms $\propto E^2$ and using partial integration and some simplifications, finally Eq. (16) of the main text is obtained.

3. Calculation of the current in 2D

Having introduced $\mathbf{u}_{\mathbf{0}}^{\mathbf{2D}}$ in the main text and following an identical derivation to Sec. B 2 the results in 2D for the nonlinear response reads:

$$\begin{aligned} J_\alpha^{(2)}(t) = & -e^2 \int \frac{d^2k}{(2\pi)^2} D(\mathbf{k}) \mathbf{u}_{\mathbf{0}\alpha}^{\mathbf{2D}}(\mathbf{k}) \left[\frac{\partial f_0(\varepsilon(\mathbf{k}_0(t)))}{\partial \varepsilon} \int_{-\infty}^{t} dt' \sum_{\beta\gamma} E_\beta(t) k_{1\gamma}(t') \frac{\partial}{\partial k_\gamma} \left[D^{-1}(\mathbf{k}_0(t')) \frac{\partial}{\partial k_\beta} \varepsilon(\mathbf{k}_0(t')) \right] \eta(t;t') \right. \\ & + e \frac{\partial^2 f_0(\varepsilon(\mathbf{k}_0(t)))}{\partial \varepsilon^2} \int_{-\infty}^{t} dt' D^{-1}(\mathbf{k}_0(t')) \nabla_{\mathbf{k}} \varepsilon(\mathbf{k}_0(t)) \cdot \mathbf{E}(t') \eta(t;t') \int_{t'}^{t} D^{-1}(\mathbf{k}_0(l)) \nabla_{\mathbf{k}} \varepsilon(\mathbf{k}_0(l)) \cdot \mathbf{E}(l) dl \end{aligned}$$

$$+\frac{\partial f_0(\varepsilon(\mathbf{k}_0(t)))}{\partial\varepsilon}\int_{-\infty}^{t} dt' D^{-1}(\mathbf{k}_0(t'))\nabla_{\mathbf{k}}\varepsilon(\mathbf{k}_0(t'))\cdot\mathbf{E}(t')\eta(t;t')\int_{t'}^{t}\frac{\nabla_{\mathbf{k}}\tau_S(\mathbf{k}_0(l))\cdot\mathbf{k}_1(l)}{\tau_S^2(\mathbf{k}_0(l))}dl\Bigg]$$
$$-e^3\varepsilon_{\alpha\beta}\int\frac{d^2k}{(2\pi)^2}E_\beta(t)\Omega(\mathbf{k})\cdot\frac{\partial f_0(\varepsilon(\mathbf{k}))}{\partial\varepsilon}\int_{-\infty}^{t} dt' D^{-1}(\mathbf{k}_0(t'))\nabla_{\mathbf{k}}\varepsilon(\mathbf{k}_0(t'))\cdot\mathbf{E}(t')\eta(t;t'). \tag{B3}$$

APPENDIX C: HALL COEFFICIENT CALCULATIONS FOR RECTANGULAR LATTICE

In Ref. [56] the authors have solved Boltzmann transport equations for this energy dispersion analytically. Then they calculated the velocities u_x and u_y and took their Fourier series expansions, which are shown below:

$$u^i_{0x}(t) = (1-2\delta_{i,h})\frac{2\pi}{m_0K(\kappa)}\sum_{n=1}^{\infty}\operatorname{sech}\left[\frac{(2n-1)\pi K'}{2K(\kappa)}\right]\sin\left[\frac{(2n-1)\pi u_i}{2K(\kappa)}\right]\sin\left[\frac{(2n-1)\pi\omega_0 t}{2K(\kappa)}\right], \tag{C1}$$

$$u^i_{0y}(t) = \frac{2\pi}{m_0K(\kappa)}\sum_{n=1}^{\infty}\operatorname{sech}\left[\frac{(2n-1)\pi K'}{2K(\kappa)}\right]\cos\left[\frac{(2n-1)\pi u_i}{2K(\kappa)}\right]\cos\left[\frac{(2n-1)\pi\omega_0 t}{2K(\kappa)}\right], \tag{C2}$$

where $i = e$ for electrons and $i = h$ for holes. For open surfaces the corresponding results are:

$$u^o_{0x}(t) = \frac{2\pi\kappa}{m_0K(1/\kappa)}\sum_{n=1}^{\infty}\operatorname{sech}\left[\frac{n\pi K'}{K(1/\kappa)}\right]\sin\left[\frac{n\pi u_o}{K(1/\kappa)}\right]\sin\left[\frac{n\pi\kappa\omega_0 t}{K(1/\kappa)}\right], \tag{C3}$$

$$u^o_{0y}(t) = \frac{2\pi\kappa}{m_0K(1/\kappa)}\left\{\frac{1}{2}+\sum_{n=1}^{\infty}\operatorname{sech}\left[\frac{n\pi K'}{K(1/\kappa)}\right]\cos\left[\frac{n\pi u_o}{K(1/\kappa)}\right]\cos\left[\frac{n\pi\kappa\omega_0 t}{K(1/\kappa)}\right]\right\}, \tag{C4}$$

where the definitions of m_0, κ, ω_0, K, and K' are given in the main text.

For electron and hole pockets we can write for simplicity:

$$u_{0x}(t) = \tilde{u}_x\sum_{n=1}^{\infty}a^x_n\sin\left[\frac{(2n-1)\pi\omega_0 t}{2K(\kappa)}\right], \tag{C5}$$

$$u_{0y}(t) = \tilde{u}_y\sum_{n=1}^{\infty}a^y_n\cos\left[\frac{(2n-1)\pi\omega_0 t}{2K(\kappa)}\right]. \tag{C6}$$

Equation (17) is also true for open surfaces. But in the case of $u_y(t)$ we should write

$$u^o_x(t) = \tilde{u}_x\sum_{n=1}^{\infty}a^x_n\sin\left[\frac{n\pi\kappa\omega_0 t}{K(1/\kappa)}\right], \tag{C7}$$

$$u^o_y(t) = \tilde{u}_y\left\{\frac{1}{2}+\sum_{n=1}^{\infty}a^y_n\cos\left[\frac{n\pi\kappa\omega_0 t}{K(1/\kappa)}\right]\right\}. \tag{C8}$$

Both for holes and electrons the results read for closed Fermi surfaces:

$$\sigma_{xy} = \frac{e^3B}{(2\pi)^2}\int_0^{4K/\omega_0}\tilde{u}_x\sum_{n=1}^{\infty}a^x_n\sin\left[\frac{(2n-1)\pi\omega_0 t}{2K(\kappa)}\right]dt\int_{-\infty}^{t}\tilde{u}_y\sum_{m=1}^{\infty}a^y_m\cos\left[\frac{(2m-1)\pi\omega_0 t'}{2K(\kappa)}\right]\exp\{-[1/\tau_S+i\omega](t-t')\}dt'$$
$$= \frac{e^3B}{4\pi}\tilde{u}_x\tilde{u}_y\sum_{n=1}^{\infty}a^x_n a^y_n\frac{2n-1}{[1/\tau_S+i\omega]^2+\left[\frac{(2n-1)\pi\omega_0}{2K(\kappa)}\right]^2}, \tag{C9}$$

$$\sigma_{xx} = \frac{e^3B}{(2\pi)^2}\int_0^{4K/\omega_0}\tilde{u}_x\sum_{n=1}^{\infty}a^x_n\sin\left[\frac{(2n-1)\pi\omega_0 t}{2K(\kappa)}\right]dt\int_{-\infty}^{t}\tilde{u}_x\sum_{m=1}^{\infty}a^x_m\sin\left[\frac{(2m-1)\pi\omega_0 t'}{2K(\kappa)}\right]\exp\left(-[1/\tau_S+i\omega](t-t')\right)dt'$$
$$= \frac{e^3B}{(2\pi)^2}\tilde{u}_x^2\sum_{n=1}^{\infty}(a^x_n)^2\frac{[1/\tau_S+i\omega]}{[1/\tau_S+i\omega]^2+\left[\frac{(2n-1)\pi\omega_0}{2K(\kappa)}\right]^2}\frac{2K(\kappa)}{\omega_0}, \tag{C10}$$

$$\sigma_{yy} = \frac{e^3B}{(2\pi)^2}\int_0^{4K/\omega_0}\tilde{u}_y\sum_{n=1}^{\infty}a^y_n\cos\left[\frac{(2n-1)\pi\omega_0 t}{2K(\kappa)}\right]dt\int_{-\infty}^{t}\tilde{u}_y\sum_{m=1}^{\infty}a^y_m\cos\left[\frac{(2m-1)\pi\omega_0 t'}{2K(\kappa)}\right]\exp\left(-[1/\tau_S+i\omega](t-t')\right)dt'$$
$$= \frac{e^3B}{(2\pi)^2}\tilde{u}_y^2\sum_{n=1}^{\infty}\left(a^y_n\right)^2\frac{[1/\tau_S+i\omega]}{[1/\tau_S+i\omega]^2+\left[\frac{(2n-1)\pi\omega_0}{2K(\kappa)}\right]^2}\frac{2K(\kappa)}{\omega_0}. \tag{C11}$$

For open Fermi surfaces:

$$\sigma_{xx} = \frac{e^3B}{(2\pi)^2}\int_0^{4K/\kappa\omega_0}\tilde{u}_x\sum_{n=1}^{\infty}a_n^x\sin\left[\frac{n\pi\kappa\omega_0 t}{K(1/\kappa)}\right]dt\int_{-\infty}^{t}\tilde{u}_x\sum_{m=1}^{\infty}a_m^x\sin\left[\frac{m\pi\kappa\omega_0 t}{K(1/\kappa)}\right]\exp\left(-[1/\tau_S+i\omega](t-t')\right)dt'$$

$$= \frac{e^3B}{(2\pi)^2}\tilde{u}_x^2\sum_{n=1}^{\infty}\left(a_n^x\right)^2\frac{[1/\tau_S+i\omega]}{[1/\tau_S+i\omega]^2+\left[\frac{n\pi\kappa\omega_0}{K(1/\kappa)}\right]^2}\frac{K(1/\kappa)}{\kappa\omega_0}, \tag{C12}$$

$$\sigma_{xy} = \frac{e^3B}{(2\pi)^2}\int_0^{4K/\kappa\omega_0}\tilde{u}_x\sum_{n=1}^{\infty}a_n^x\sin\left[\frac{n\pi\kappa\omega_0 t}{K(1/\kappa)}\right]dt\int_{-\infty}^{t}\tilde{u}_y\left\{\frac{1}{2}+\sum_{m=1}^{\infty}a_m^y\cos\left[\frac{m\pi\kappa\omega_0 t}{K(1/\kappa)}\right]\right\}\exp\left(-[1/\tau_S+i\omega](t-t')\right)dt'$$

$$= \frac{e^3B}{(2\pi)^2}\tilde{u}_x\tilde{u}_y\sum_{n=1}^{\infty}a_n^x a_n^y\frac{n\pi}{[1/\tau_S+i\omega]^2+\left[\frac{n\pi\kappa\omega_0}{K(1/\kappa)}\right]^2}, \tag{C13}$$

$$\sigma_{yy} = \frac{e^3B}{(2\pi)^2}\int_0^{4K/\kappa\omega_0}\tilde{u}_y\left\{\frac{1}{2}+\sum_{n=1}^{\infty}a_n^y\cos\left[\frac{n\pi\kappa\omega_0 t}{K(1/\kappa)}\right]\right\}dt\int_{-\infty}^{t}\tilde{u}_y\left\{\frac{1}{2}+\sum_{m=1}^{\infty}a_m^y\cos\left[\frac{m\pi\kappa\omega_0 t}{K(1/\kappa)}\right]\right\}\exp\left(-[1/\tau_S+i\omega](t-t')\right)dt'$$

$$= \frac{e^3B}{(2\pi)^2}\frac{\tilde{u}_y^2}{[1/\tau_S+i\omega]}\frac{K(1/\kappa)}{\kappa\omega_0}+\frac{e^3B}{(2\pi)^2}\tilde{u}_y^2\sum_{n,1}^{\infty}\left(a_n^y\right)^2\frac{[1/\tau_S+i\omega]}{[1/\tau_S+i\omega]^2+\left[\frac{n\pi\kappa\omega_0}{K(1/\kappa)}\right]^2}\frac{K(1/\kappa)}{\kappa\omega_0}. \tag{C14}$$

From which if $\tilde{u}_x$, $\tilde{u}_y$, a_n^x, a_n^y are substituted, Eqs. (26), (27), and (28) follow. As we emphasized in the main text, the sums are over positive odd integers while for open surfaces the sums are over positive even integers.

1. Hall coefficient for rectangular lattice at limiting cases

For the high-field limit:

$$\frac{1}{R_H} = \lim_{B\to\infty}\frac{1}{B}\frac{\sigma_{xy}}{\sigma_{xx}\sigma_{yy}+\sigma_{xy}^2} \tag{C15}$$

Using the above equations, we obtain:

$$R_H^e = -\frac{1}{\pi}\sum_{n=1}^{\infty}\frac{1}{\left(n-\frac{1}{2}\right)}\mathrm{sech}^2\left[\left(n-\frac{1}{2}\right)\frac{\pi K'(\kappa)}{K(\kappa)}\right]\sin\left[(2n-1)\frac{\pi u_e}{K(\kappa)}\right], \tag{C16}$$

$$R_H^h = \frac{1}{\pi}\sum_{n=1}^{\infty}\frac{1}{\left(n-\frac{1}{2}\right)}\mathrm{sech}^2\left[\left(n-\frac{1}{2}\right)\frac{\pi K'(\kappa)}{K(\kappa)}\right]\sin\left[(2n-1)\frac{\pi u_h}{K(\kappa)}\right], \tag{C17}$$

$$R_H^o = -\frac{1}{\pi}\frac{\sum_{n=1}^{\infty}\frac{1}{n^2}\mathrm{sech}^2\left[\frac{n\pi K'(1/\kappa)}{K(1/\kappa)}\right]\sin^2\left[\frac{n\pi u_o}{K(1/\kappa)}\right]}{\sum_{n=1}^{\infty}\frac{1}{2n}\mathrm{sech}^2\left[\frac{n\pi K'(1/\kappa)}{K(1/\kappa)}\right]\sin\left[\frac{2n\pi u_o}{K(1/\kappa)}\right]}-\frac{1}{\pi}\sum_{n=1}^{\infty}\frac{1}{n}\mathrm{sech}^2\left[\frac{n\pi K'(1/\kappa)}{K(1/\kappa)}\right]\sin\left[\frac{2n\pi u_o}{K(1/\kappa)}\right], \tag{C18}$$

and we observe that in the high-field case the Hall number does not depend on the frequency. Similarly, for the low-field case the formulas are:

$$\frac{1}{R_H} = \lim_{B\to 0}\frac{1}{B}\frac{\sigma_{xy}}{\sigma_{xx}\sigma_{yy}+\sigma_{xy}^2}, \tag{C19}$$

similarly we get:

$$R_H^e = -\frac{4}{\pi}\frac{\left[\sum_{n=1}^{\infty}\mathrm{sech}^2\left[\left(n-\frac{1}{2}\right)\frac{\pi K'}{K}\right]\sin^2\left[\left(n-\frac{1}{2}\right)\frac{\pi u_e}{K}\right]\right]\left[\sum_{n=1}^{\infty}\mathrm{sech}^2\left[\left(n-\frac{1}{2}\right)\frac{\pi K'}{K}\right]\cos^2\left[\left(n-\frac{1}{2}\right)\frac{\pi u_e}{K}\right]\right]}{\sum_{n=1}^{\infty}\left(n-\frac{1}{2}\right)\mathrm{sech}^2\left[\left(n-\frac{1}{2}\right)\frac{\pi K'}{K}\right]\sin\left[\frac{(2n-1)\pi u_e}{K}\right]}, \tag{C20}$$

$$R_H^h = \frac{4}{\pi}\frac{\left[\sum_{n=1}^{\infty}\mathrm{sech}^2\left[\left(n-\frac{1}{2}\right)\frac{\pi K'}{K}\right]\sin^2\left[\left(n-\frac{1}{2}\right)\frac{\pi u_h}{K}\right]\right]\left[\sum_{n=1}^{\infty}\mathrm{sech}^2\left[\left(n-\frac{1}{2}\right)\frac{\pi K'}{K}\right]\cos^2\left[\left(n-\frac{1}{2}\right)\frac{\pi u_h}{K}\right]\right]}{\sum_{n=1}^{\infty}\left(n-\frac{1}{2}\right)\mathrm{sech}^2\left[\left(n-\frac{1}{2}\right)\frac{\pi K'}{K}\right]\sin\left[\frac{(2n-1)\pi u_h}{K}\right]}, \tag{C21}$$

$$R_H^o = -\frac{4}{\pi}\frac{\left[\sum_{n=1}^{\infty}\mathrm{sech}^2\left[\frac{n\pi K'}{K}\right]\sin^2\left[\frac{n\pi u_o}{K}\right]\right]\left[\frac{1}{2}+\sum_{n=1}^{\infty}\mathrm{sech}^2\left[\frac{n\pi K'}{K}\right]\cos^2\left[\frac{n\pi u_o}{K}\right]\right]}{\sum_{n=1}^{\infty}n\,\mathrm{sech}^2\left[\frac{n\pi K'}{K}\right]\sin\left[\frac{2n\pi u_o}{K}\right]}. \tag{C22}$$

APPENDIX D: SOLUTION TO RELEVANT ORDINARY DIFFERENTIAL EQUATIONS (ODEs)

1. General setup

Equation (13) is of the general form:

$$\frac{d\mathbf{X}}{dt} = M(t)\mathbf{X} + \mathbf{V}(t). \tag{D1}$$

First we need to solve for

$$\frac{d\mathbf{X}_0}{dt} = M(t)\mathbf{X}_0, \tag{D2}$$

where

$$\mathbf{X}_0(t) = T\left(\exp\left(\int_{t_0}^{t} M(s)ds\right)\right)\mathbf{X}_0(t_0). \tag{D3}$$

Here T stands for time ordering. Then, for Eq. (D1), we look for solutions of the form

$$\begin{aligned}
\mathbf{X}(t) &= T\left(\exp\left(\int_{t_0}^{t} M(s)ds\right)\right)\mathbf{Y}(t),\\
\frac{d\mathbf{X}(t)}{dt} &= M(t)\mathbf{X}(t) + T\left(\exp\left(\int_{t_0}^{t} M(s)ds\right)\right)\frac{d\mathbf{Y}(t)}{dt}\\
&\equiv M(t)\mathbf{X} + \mathbf{V}(t),\\
\Rightarrow \frac{d\mathbf{Y}(t)}{dt} &= T\left(\exp\left(\int_{t_0}^{t} M(s)ds\right)\right)^{-1}\mathbf{V}(t),\\
\mathbf{Y}(t) &= \mathbf{Y}_0 + \int_{t_0}^{t} T\left(\exp\left(\int_{t_0}^{t'} M(s)ds\right)\right)^{-1}\mathbf{V}(t')dt'.
\end{aligned} \tag{D4}$$

2. Solution of Eq. (A8) in 3D

We use the results of Appendix D 1. In our case $\mathbf{Y}_0 = 0$ and

$$\mathbf{k}_1(t) = \int_{t_0}^{t} T\left(\exp\left(\int_{t'}^{t} M(s)ds\right)\right)\mathbf{V}(t')dt' \tag{D5}$$

where $\mathbf{V}(t') = -e\mathbf{E}(t')$ and

$$M_{\alpha\beta}(s) = -e\sum_{\gamma\delta}\varepsilon_{\alpha\gamma\delta}B_\delta\frac{\partial^2}{\partial k_\beta \partial k_\gamma}\varepsilon(\mathbf{k}_0(s)). \tag{D6}$$

Then, for $t > t_0$:

$$\mathbf{k}_1(t) = -\int_{t_0}^{t} T\left(\exp\left(\int_{t'}^{t} M(s)ds\right)\right)^{-1}\mathbf{V}(t')dt'.$$

3. Solution of Eq. (13) in 3D

Then $\mathbf{Y}_0 = 0$ and for $t > t_0$

$$\mathbf{k}_1(t) = \int_{t_0}^{t} T\left(\exp\left(\int_{t'}^{t} M(s)ds\right)\right)\mathbf{V}(t')dt'. \tag{D7}$$

In addition:

$$\mathbf{V}(t') = -D^{-1}(\mathbf{k}_0(t'))[e\mathbf{E}(t') + e^2(\mathbf{B}\cdot\mathbf{E}(t'))\boldsymbol{\Omega}(\mathbf{k}_0(t'))], \tag{D8}$$

and

$$M_{\alpha\beta}(s) = -e\sum_{\gamma\delta}\varepsilon_{\alpha\gamma\delta}B_\delta\frac{\partial}{\partial k_\beta}\left[D^{-1}(\mathbf{k}_0(s))\left[\frac{\partial}{\partial k_\gamma}\varepsilon_M(\mathbf{k}_0(s))\right]\right], \tag{D9}$$

therefore for $t > t_0$

$$\mathbf{k}_1(t) = -\int_{t_0}^{t} T\left(\exp\left(\int_{t}^{t'} M(s)ds\right)\right)^{-1}\mathbf{V}(t')dt'. \tag{D10}$$

We note that the perturbative correction in Eq. (A17), $\mathbf{k}_1(l)$ is linear in the external electric field as can be seen by Eqs. (D8), (D9), and (D10). As a result, these terms are well convergent for small electric fields. Due to the time ordered exponential in Eq. (D9) though, there may be limitation to how large the eigenvalues of the matrix in Eq. (D9) can be. The reason is that although there is a damping exponential $\eta(t;t_0)$, which makes various integrals convergent while the exponential in Eq. (D10) can lead to divergences. Therefore, it is important that the damping term is greater that the divergent one and as such the eigenvalues of the matrix in Eq. (D9) need to be smaller then $\frac{1}{\tau_S(\mathbf{k})}$.

4. Solution of equations in 2D

In a similar way we've got $\mathbf{Y}_0 = 0$ and for $t > t_0$

$$\mathbf{k}_1(t) = \int_{t_0}^{t} T\left(\exp\left(\int_{t'}^{t} M(s)ds\right)\right)\mathbf{V}(t')dt'. \tag{D11}$$

We also have that: $\mathbf{V}(t') = -eD^{-1}(\mathbf{k}_0(t'))\mathbf{E}(t')$ and

$$M_{\alpha\beta}(s) = -e\sum_{\gamma}\varepsilon_{\alpha\gamma}B\frac{\partial}{\partial k_\beta}\left[D^{-1}(\mathbf{k}_0(s))\left[\frac{\partial}{\partial k_\gamma}\varepsilon_M(\mathbf{k}_0(s))\right]\right]. \tag{D12}$$

Therefore for $t > t_0$ the solution reads:

$$\mathbf{k}_1(t) = -\int_{t_0}^{t} T\left(\exp\left(\int_{t}^{t'} M(s)ds\right)\right)^{-1}\mathbf{V}(t')dt'. \tag{D13}$$

[1] J. M. Ziman, *Principles of the Theory of Solids* (Cambridge University Press, Cambridge, 1972).

[2] A. A. Abrikosov, *Fundamentals of the Theory of Metals* (North Holland, Amsterdam, 1988).

[3] L. Van Hove, Phys. Rev. **89**, 1189 (1953).

[4] I. M. Lifshitz, Zh. Eksp. Teor. Fiz. **38**, 1569 (1960) [Sov. Phys. JETP **11**, 1130 (1960)].

[5] A. Chandrasekaran, A. Shtyk, J. J. Betouras, and C. Chamon, Phys. Rev. Research **2**, 013355 (2020).

[6] A. Chandrasekaran and J. J. Betouras, Phys. Rev. B **105**, 075144 (2022).

[7] A. I. Coldea, S. F. Blake, S. Kasahara, A. A. Haghighirad, M. D. Watson, W. Knafo, E. S. Choi, A. McCollam, P. Reiss, T. Yamashita *et al.*, npj Quantum Mater. **4**, 2 (2019).

[8] Y. Okamoto, A. Nishio, and Z. Hiroi, Phys. Rev. B **81**, 121102(R) (2010).

[9] E. A. Yelland, J. M. Barraclough, W. Wang, K. V. Kamenev, and A. D. Huxley, Nat. Phys. **7**, 890 (2011).

[10] S. N. Khan and D. D. Johnson, Phys. Rev. Lett. **112**, 156401 (2014).

[11] S. Benhabib, A. Sacuto, M. Civelli, I. Paul, M. Cazayous, Y. Gallais, M.-A. Measson, R. D. Zhong, J. Schneeloch, G. D. Gu, D. Colson, and A. Forget, Phys. Rev. Lett. **114**, 147001 (2015).

[12] S. Slizovskiy, A. V. Chubukov, and J. J. Betouras, Phys. Rev. Lett. **114**, 066403 (2015).

[13] D. Aoki, G. Seyfarth, A. Pourret, A. Gourgout, A. McCollam, J. A. N. Bruin, Y. Krupko, and I. Sheikin, Phys. Rev. Lett. **116**, 037202 (2016).

[14] Y. Sherkunov, A. V. Chubukov, and J. J. Betouras, Phys. Rev. Lett. **121**, 097001 (2018).

[15] Y. Sherkunov and J. J. Betouras, Phys. Rev. B **98**, 205151 (2018).

[16] M. E. Barber, F. Lechermann, S. V. Streltsov, S. L. Skornyakov, S. Ghosh, B. J. Ramshaw, N. Kikugawa, D. A. Sokolov, A. P. Mackenzie, C. W. Hicks, and I. I. Mazin, Phys. Rev. B **100**, 245139 (2019).

[17] I. Stewart, Rep. Prog. Phys. **45**, 185 (1982).

[18] D. V. Efremov, A. Shtyk, A. W. Rost, C. Chamon, A. P. Mackenzie, and J. J. Betouras, Phys. Rev. Lett. **123**, 207202 (2019).

[19] P. Rosenzweig, H. Karakachian, D. Marchenko, K. Kuster, and U. Starke, Phys. Rev. Lett. **125**, 176403 (2020).

[20] N. F. Q. Yuan and L. Fu, Phys. Rev. B **101**, 125120 (2020).

[21] N. F. Q. Yuan, H. Isobe, and L. Fu, Nat. Commun. **10**, 5769 (2019).

[22] H. Isobe and L. Fu, Phys. Rev. Res. **1**, 033206 (2019)

[23] H. Zhou, L. Holleis, Y. Saito, L. Cohen, W. Huynh, C. L. Patterson, F. Yang, T. Taniguchi, K. Watanabe, and A. F. Young, Science **375**, 6582 (2021).

[24] A. Shtyk, G. Goldstein, and C. Chamon, Phys. Rev. B **95**, 035137 (2017).

[25] R. G. Chambers, Proc. Phys. Soc. A **65**, 458 (1952).

[26] W. Shockley, Phys. Rev. **79**, 191 (1950).

[27] J. Callaway, *Quantum Theory of the Solid State* (Academic Press, Boston, 1991).

[28] J. M. Ziman, *Electrons and Phonons: The Theory of Transport of Solids* (Oxford University Press, Oxford, 1960).

[29] C. Kittel, *Quantum Theory of Solids* (John Wiley & Sons, New York, 1987).

[30] N. Singh, *Electronic Transport Theories: From Wekaly to Strongly Correlated Materials* (Taylor & Francis, Boca Raton, 2017).

[31] W. Jones and N. H. March, *Theoretical Solid State Physics (Volume 2): Non-Equilibrium and Disorder* (John Wiley & Sons, London, 1973).

[32] A. H. Wilson, *The Theory of Metals* (Cambridge University Press, Cambridge, 1953).

[33] Y. M. Galperin, *Introduction to Modern Solid State Physics* (CreateSpace Independent Publishing Platform, 2014).

[34] J. J. Quinn and K. S. Yi, *Solid State Physics: Principles and Modern Applications* (Springer-Verlag, Berlin, 2009).

[35] Y. Gao, Front. Phys. **14(3)**, 33404 (2019).

[36] Y. Gao, S. A. Yang, and Q. Niu, Phys. Rev. Lett. **112**, 166601 (2014).

[37] D. Xiao, M.-C. Chang, and Q. Niu, Rev. Mod. Phys. **82**, 1959 (2010).

[38] D. Xiao, J. Shi, and Q. Niu, Phys. Rev. Lett. **95**, 137204 (2005).

[39] D. Xiao, Y. Yao, Z. Fang, and Q. Niu, Phys. Rev. Lett. **97**, 026603 (2006).

[40] D. Vanderbilt, *Berry Phases in Electronic Structure Theory: Electric Polarization, Orbital Magnetization and Topological Insulators* (Cambridge University Press, Cambridge, 2018).

[41] I. Sodemann and L. Fu, Phys. Rev. Lett. **115**, 216806 (2015).

[42] J. I. Facio, D. V. Efremov, K. Koepernik, J.-S. You, I. Sodemann, and J. van den Brink, Phys. Rev. Lett. **121**, 246403 (2018).

[43] L. M. Falicov and P. R. Sievert, Phys. Rev. **138**, A88 (1965).

[44] A. Alexandradinata and L. Glazman, Phys. Rev. Lett. **119**, 256601 (2017).

[45] E. Deyo, L. E. Golub, E. L. Ivchenko, and B. Spivak, arXiv:0904.1917.

[46] G. Sundaram and Q. Niu, Phys. Rev. B **59**, 14915 (1999).

[47] M. C. Chang and Q. Niu, Phys. Rev. Lett. **75**, 1348 (1995).

[48] M. C. Chang and Q. Niu, Phys. Rev. B **53**, 7010 (1996).

[49] M. C. Chang and Q. Niu, J. Phys.: Condens. Matter **20**, 193202 (2008).

[50] D. Arovas, *Lecture Notes in Condensed Matter Physics (A Work in Progress)* (CreateSpace Independent Publishing Platform, 2014).

[51] K.-S. Kim, H.-J. Kim, and M. Sasaki, Phys. Rev. B **89**, 195137 (2014).

[52] C. MacCallum, Phys. Rev. **132**, 930 (1963).

[53] W. R. Young, Pertubation Theory (unpublished).

[54] S. M. Bauer, S. Fillipov, A. L. Smirnov, P. E. Tovstik, and R. Villancourt, *Asymptotic Methods in Mechanics of Solids* (Springer International Publishing, Switzerland, 2015).

[55] A. H. Nayfeh, *Pertubation Methods* (John-Wiley, Hoboken, 1973).

[56] A. V. Maharaj, I. Esterlis, Y. Zhang, B. J. Ramshaw, and S. A. Kivelson, Phys. Rev B **96**, 045132 (2017).

[57] A. Auerbach, Phys. Rev. Lett. **121**, 066601 (2018).